論文 / 著書情報
Article / Book Information

題目(和文)	
Title(English)	Design of coiled-coil based biomaterials for therapeutic applications
著者(和文)	ASSALYasmine
Author(English)	Yasmine Assal
出典(和文)	学位:博士(学術), 学位授与機関:東京工業大学, 報告番号:甲第9343号, 授与年月日:2013年9月25日, 学位の種別:課程博士, 審査員:小畠 英理,十川 久美子,山口 雄輝,有坂 文雄,小倉 俊一郎
Citation(English)	Degree:Doctor (Academic), Conferring organization: Tokyo Institute of Technology, Report number:甲第9343号, Conferred date:2013/9/25, Degree Type:Course doctor, Examiner:,,,,
学位種別(和文)	博士論文
Type(English)	Doctoral Thesis

TOKYO INSTITUTE OF TECHNOLOGY

Design of coiled-coil based biomaterials for therapeutic applications

Supervised by Eiry Kobatake

Professor, Tokyo Institute of Technology

Submitted in total conformity with the requirements

for the degree of Doctor of Philosophy

By

Yasmine ASSAL

Department of Biological Information

Graduate School of Bioscience and Biotechnology

Tokyo Institute of Technology

September 2013

Table of Contents

Chapter 1: General introduction

Chapter 2: The promotion of angiogenesis by growth factors integrated with ECM proteins through coiled-coil structures

Chapter 3: Nanoparticle-Growth factor interaction through coiled-coil formation: A promising biomaterial for targeted drug delivery

List of Abbreviations

ELPs:	Elastin-like polypeptides
ECM:	Extracellular matrix
RGD:	aginine- glycine- aspartic acid
IKVAV:	isoleucine- lysine- valine- alanine- valine
APGVGV:	arginine- proline- glycine- valine- glycine- valine
E:	APGVGV repeats
CBD:	Collagen binding domain
fn:	Fibronectin
GF:	Growth factor
ACID-p1:	helixA
BASE-p1:	helixB
VEGF:	Vascular endothelial growth factor
EGF:	Epidermal growth factor
bFGF:	Basic fibroblast growth factor
VEGF-R:	VEGF receptors
HUVECs:	Human umbilical vein endothelial cells
A:	Atelocollagen
ACF:	Atelocollagen+CBDEREI2-helixB+helixA-bFGF
ACFE:	Atelocollagen+CBDEREI2-helixB+helixA-bFGF+helix-EGF
ACFV:	Atelocollagen+CBDEREI2-helixB+helixA-bFGF+helixA-scVEGF121
ACFEV:	Atelocollagen+CBDEREI2-helixB+helixA-bFGF+helixA-EGF+helixA-scVEGF121
PAVGV:	proline- arginine- valine- glycine- valine
D:	Polyaspartic acid
PDB:	PAVGV repeats+ Polyaspartic acid+ helixB
1,8-ANS:	1-anilinonaphthalene-8-sulfonate
PDBV:	PAVGV repeats+ Polyaspartic acid+ helixB+ helixA-scVEGF121
PTX:	Paclitaxel

Chapter 1

General Introduction

"There is nothing more difficult to take in hand, more perilous to conduct, or more uncertain in its success, than to take the lead in the introduction of a new order of things" – Niccolo Machiavelli

1.1 Introduction

Over the past three decades, researchers have been focusing on developing protein-engineered biomimetic materials or so-called biomaterials. Controversies about biodegradability, biocompatibility and bioresistivity have been recurrently discussed. The human tissue is indeed complex and sensitive, which requires meticulous treatment. Therefore, investigations on bio-inspired polymers and peptides have been extensively scrutinized. Controlled polymerization using genetic engineering has led to major discoveries (Figure 1) [1]. Advances in protein engineering initiated outstanding findings in tissue engineering resulting for instance in reproducing liver, artificial lung branches or microvessels [2-4].

For the construction of protein-based biomaterials, various proteins and peptides were exploited. One of the peptides, elastin-like polypeptides (ELPs), has been genetically engineered with precisely controlled sequences, molecular weights, and gelation temperatures to create protein-based biomaterials.

The increase use of ELPs as improved scaffold-based technique was due to many factors turning this polypeptide a facile tool for tissue engineering and drug delivery system. First of all, ELPs can easily be genetically encoded from synthetic gene. Second, ELPs are easily expressed and purified from *Escherichia coli* to fairly high yield. And last, ELPs can mimick viscoelasticity properties of native elastin upon crosslinking. Because of their biocompatibility, biodegradability and non-immunogeneticity, ELPs have gained huge interest in tissue engineering field and especially in design of protein-based biomaterials. Putting it all together, ELPs appear to be the suitable candidates as an extracellular matrix (ECM) and drug carrier polypeptides. However, tissue repair often requires not only a suitable ECM but also growth factors to enhance cell proliferation and induce cell differentiation.

Then again, drug delivery system frequently requires a biodegradable carrier along with a growth factor appended at its end for cell-specific recognition. Therefore, development of techniques to bind growth factors to ELP-based biomaterials.

This chapter will focus on biomaterials for tissue engineering and drug delivery system based on elastin-like polypeptides. The significance of non-covalent binding based

approach for tethering growth factors to ELPs using fusion proteins and the description of the purpose of this study will be highlighted later on.

1.2 ELP-based biomaterials

Matrix remodeling is crucial for neovascularization, however its utilization to control this process in synthetic biomaterials is limited. Fibronectin, laminin, vitronectin, tenascin, collagen and elastin in granulation tissue and in endothelial basement membrane are indispensable for endothelial cell migration and development of new capillary tubule structures. Hyaluronic acid (HA) hydrogels, elastin-like polypeptides and collagen matrices have been engineered not only to replicate biological properties of native extracellular matrices but also to spatially control cellular remodeling during vascuslar network formation [5-7].

Along with collagen, several studies have reported exceptional properties of biomimetic scaffolds consisting of elastin-like polypeptides [8]. They mimic important features of the extracellular matrix architecture and can be finely controlled at the nano and microscale. Human elastin provides unique physical characteristics to the connective tissue in which it is found (skin, ligament, arteries and specialized cartilages) giving both strength and extensibility. Elastomeric domains and crosslinking domains provide the polypeptide with hydrophobic structure rendering it highly insoluble and viscoelastic. The potential of genetic engineering made it possible to recreate native elastin-like polypeptide by developing a repeat sequence of $(Val\text{-}Pro\text{-}X_{aa}\text{-}Y_{aa}\text{-}Gly)_n$ where X_{aa} is glycine or alanine and Y_{aa} can be any amino acid besides proline, respectively. This polymer happened to demonstrate a thermo-responsive and self-assembly properties that confer the recombinant biomaterial a stable spiral structure and easy accumulation onto hydrophobic surfaces (Figure 2) [9]. Additionally, its ability to form various platforms such as gels [10-12] (Figure 3) [13], films [14, 15], nanofibers and nanoparticles not only shows its flexibility in tissue engineering applications but also reveals its impressive potential as implants and use in drug delivery [10, 16-19].

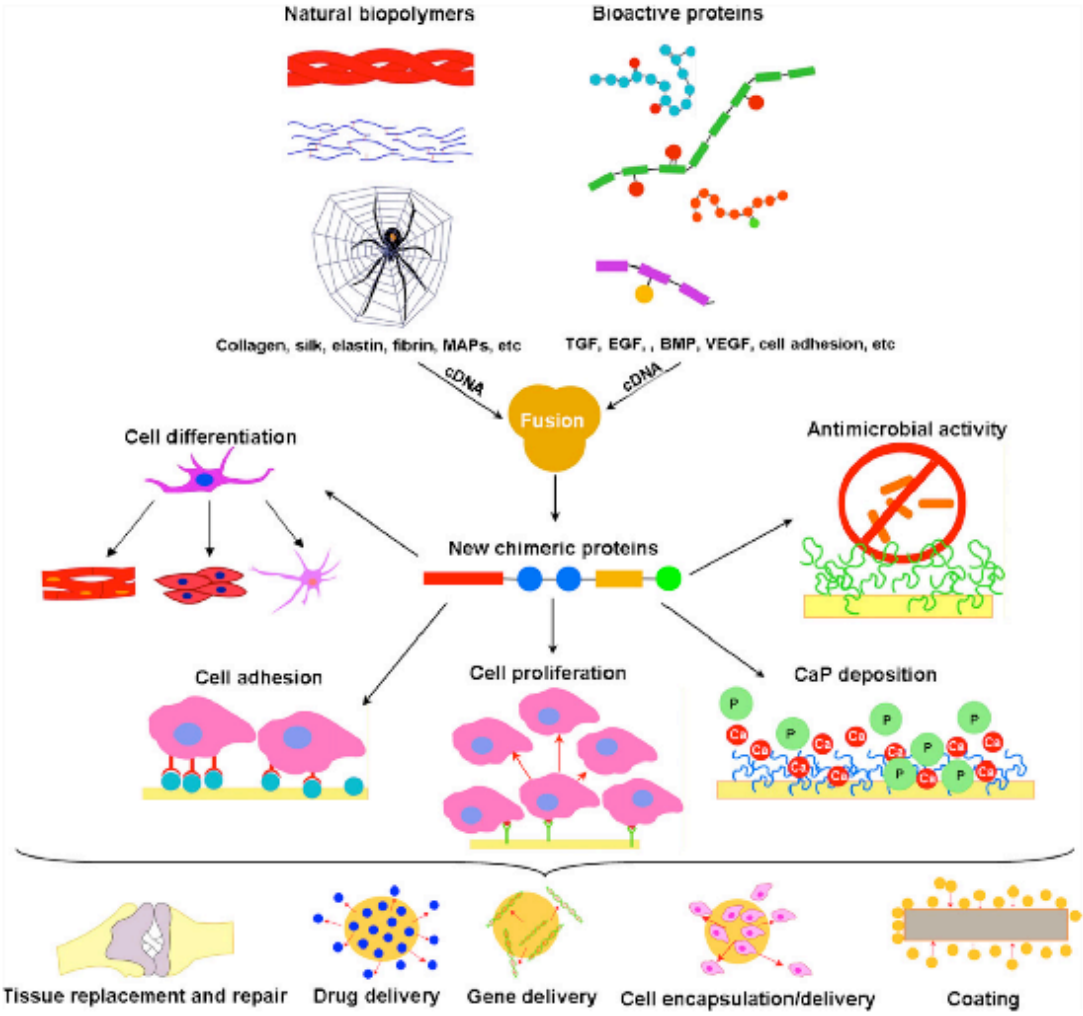

Figure 1: Scheme highlighting some of the features and applications of chimeric protein-based biomaterials synthesized through recombinant DNA technology [1].

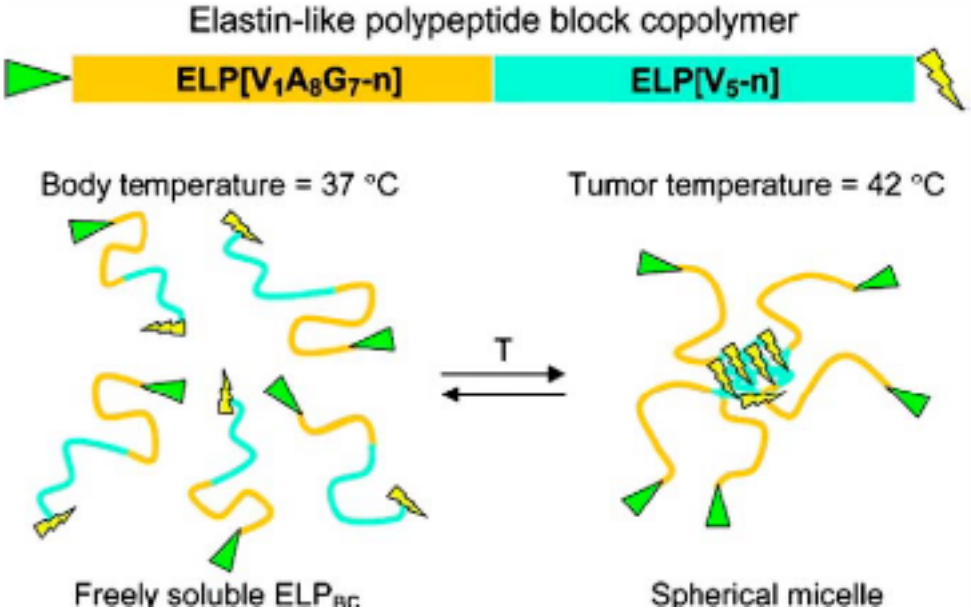

Figure 2: Temperature triggered self-assembly of an elastin like polypeptide to form polyvalent spherical micelles, which results in the presentation of a targeting ligand (green triangle) and the sequestration in the core of a drug or imaging agent (lightning bolt) [9].

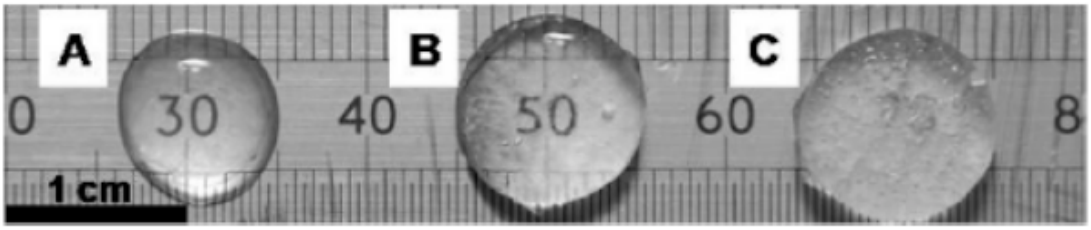

Figure 3: ELP-based hydrogel for tissue engineering. Macroscopic pictures of swollen hydrogels in water at 4 °C with different salt/polymer weight ratios: (A) 0/1, (B) 10/1, and (C) 20/1 [13].

1.1.1 ELP-based biomaterials for Tissue Engineering

Tissue engineering applications of ELP-based biomaterials are abundant and depend on the polymer design for specific applications.

Depending on ELP variants, uncrosslinked ELP have demonstrated the utility for promoting an environment encouraging chondrogenesis and led the use of coacervated ELP as a scaffold for cartilage tissue engineering. Additionally, it promoted stem cell differentiation without addition of chondrocyte-specific growth factors. On the other hand, crosslinked ELP formed turgid hydrogels leading to the synthesis of new cartilage-like matrix [20-22]. Small diameters of ELP and ELP hybrids have been studied for their potential application in vascular graft tissue engineering. Studies using ELP incorporated with cell recognition peptide sequences such as RGD sequence promoted endothelial cell adhesion. Results came out similar as if cells were coated on fibronectin substrate [23, 24].

Engineered ELP sequences containing CS5 fibronectin domain showed that cell attached on glass surfaces, promoting epithelial cell attachment, proliferation and retention of differentiated phenotype, aimed to develop naturally-derived polymer scaffolds to be used in ocular surface tissue engineering [25, 26]. Primary hepatocyte culture on ELP substratum conjugated with positively charged polyelectrolytes formed spheroids and urged cells to produce albumin and urea, two important markers of hepatocyte function, allowing hepatic tissue regeneration [27, 28].

ELPs are not cell adhesive unless combined with RGD [29, 30]. When cells mixed with RGD-containing ELP and coated on RGD-ELP surface are maintained above the transition temperature of the ELP sequence for several days and then undergo a temperature decrease below transition temperature of ELP, cells are released with their ECM as a sheet without ELP polymer. This scaffold-free cell-sheet engineering revolutionized the tissue-engineering field especially in tissue transplantation area (Figure 4) [31].

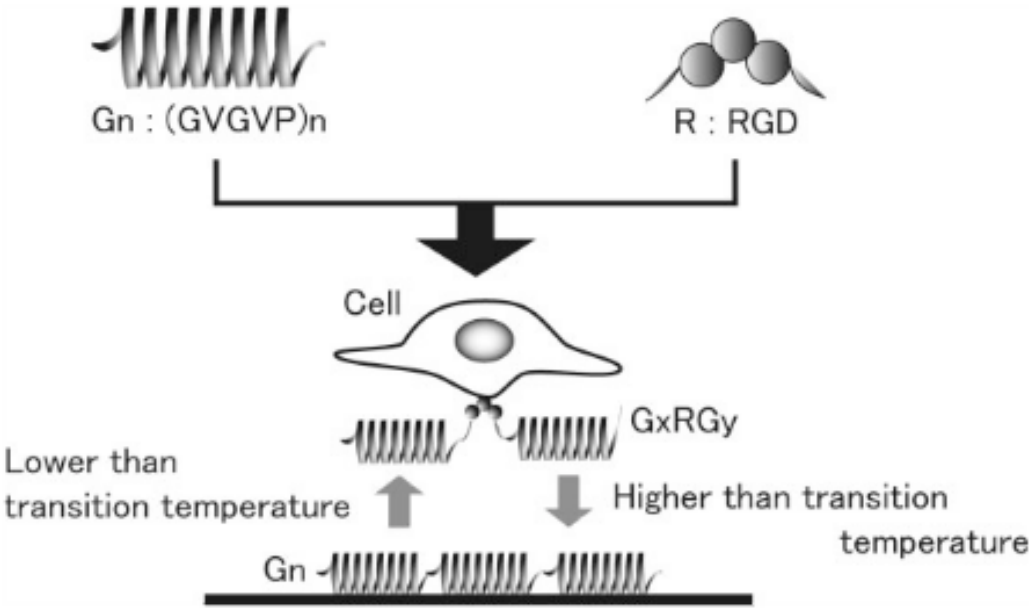

Figure 4: Schematic drawing of ELP-RGD fusion protein. Gn: n times repeat of GVGVP sequence, GxRGy: RGD sequence (R) between Gx and Gy. Gn was coated on plate followed by addition of cells with GxRGy. Gn and GXRGy were coaggreagated at 37 °C [31].

1.1.2 ELP-based biomaterials for Drug Delivery System

Targeted drug delivery using ELP polypeptides has been considerably researched due to their temperature sensitiveness, in other words, their ability to switch from hydrophilic state (below their transition temperature) to hydrophobic state (above their transition temperature). Depending on how ELPs have been genetically engineered and also on the their target delivery, ELPs are capable to undergo inverse transition [32] or maintain their particulate systems even after undercoolings [18]. This proved to confer ELPs with controlled drug release characteristics (Figure 5) [33].

Drug vehicules based on ELPs varied for instance a thermally responsive biopolymer for intra-articular drug delivery has been engineered for prolonged release of disease-modifying protein drugs for osteoarthritis and other arthritides [34]. An injectable form of ELP has been developed thanks to its lower critical solution temperature (LCST). When mixed with poly(N-isopropylacrylamide) (pNIPAAm)-based block copolymers along with drugs or cells, gel formation is observed at body temperature [35-37]. ELP injectable gels have been applied for sustained release of antiobiotics for orthopedic applications [38] or for controlled release of immunomodulator therapeutics [39] and also for the release of compounds such as vitamins [40].

Slightly similar to cell-sheet engineering, drug-eluting films can be used in medical applications as film-based implants for site-specific drug delivery applications [41] such as degradable biomedical implants [42, 43], and film coatings on medical devices [44]. ELP triblock copolymers are casted on biodegradable drug-loaded film by solvent evaporation process [12].

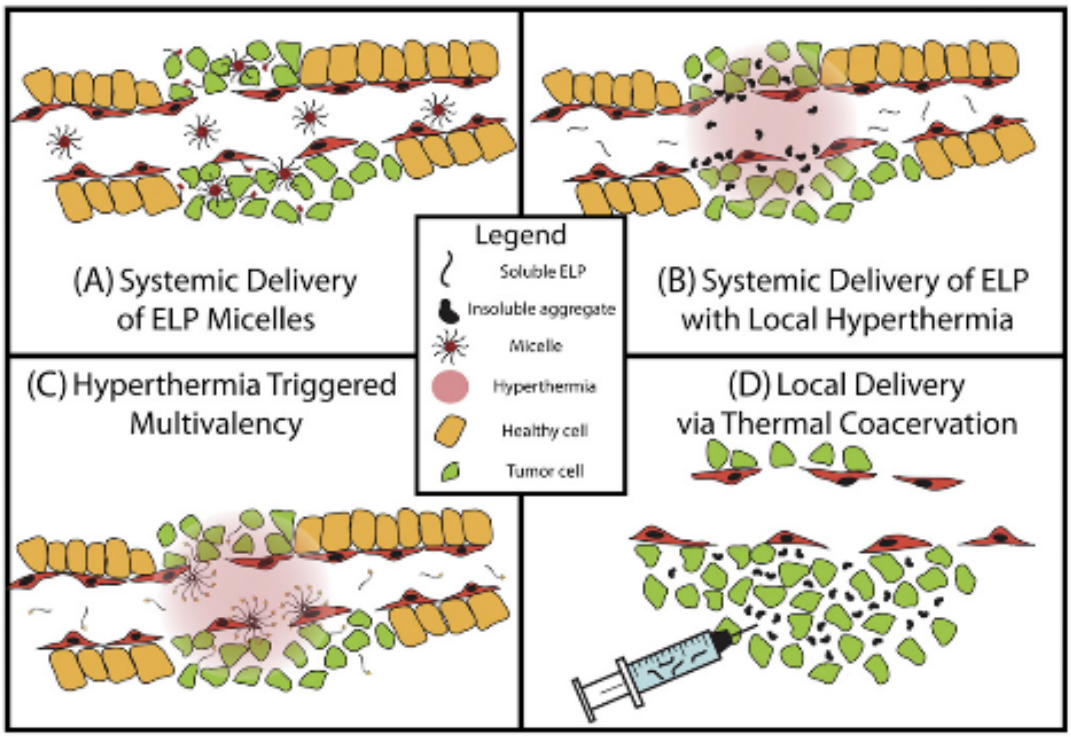

Figure 5: ELP–drug delivery strategies. This figure depicts four strategies that use ELPs to deliver drugs to a solid tumor in vivo. (A) Drug attachment triggered self-assembly of an ELP into micelles. Hydrophobic drugs are attached to the C-terminus of a hydrophilic ELP to trigger the self-assembly of micelles. These micelles accumulate in the tumor by passive diffusion through the leaky tumor vasculature. (B) Thermal targeting of an ELP to a heated tumor by the phase transition triggered aggregation of the ELP in tumor vasculature. ELP–drug conjugates can be actively targeted to a tumor by using the ELP phase transition in combination with the application of mild hyperthermia to the tumor to trigger formation of micron-sized aggregates of the ELP that adhere to the vessel walls. Upon cessation of hyperthermia, the aggregates dissolve, generating a large concentration gradient that drives the ELP that dissolves from the aggregates into the tumor. (C) Multivalent targeting of a solid tumor by thermally-triggered self-assembly of a diblock ELP into micelles in a heated tumor. (D) Local delivery of an ELP that coacervates in a solid tumor upon intratumoral injection. An ELP with a Tt below body temperature can be directly injected into a tumor to form an insoluble coacervate which forms a long-lasting depot, which extends the exposure of a conjugated radiotherapeutic to the tumor [33].

1.3 Biomaterials incorporated with growth factors

Appropriate growth factors such as vascular endothelial growth factor (VEGF), commonly known in angiogenesis activation, are needed to develop a proper environment for cell sprouting and tubular network formation [45]. Other growth factors are also used as delivery for tissue engineering like epidermal growth factor (EGF), basic fibroblast growth factor (bFGF) and platelet derived growth factor (PDGF) [46-49].

The use of VEGF in vascular tissue engineering is used in a great extend. However, its application in tumor suppression, in other words, delivering VEGF to tumor cells to trigger apoptosis is rarely mentioned. Generally, researchers fear the utilization of VEGF as it activates angiogenesis, which if not controlled, would lead to its over-expression and therefore initiates tumor angiogenesis. Usually, researchers tend to develop new techniques to block VEGF receptors (VEGF-R) or employ anti-VEGF drugs. Nonetheless in the last decade, the use of VEGF as targeting drug entity was pointed out. Studies using VEGF in a humanized docking system for drug delivery, VEGF microspheres for bone regeneration or nanoparticles bearing VEGF to enhance regeneration of decellularized tissue-engineered scaffolds have been conducted [50-52]. Additionally, nanoparticles based on biodegradable polyesters (i.e., PLGA) for the delivery of proangiogenic growth factors has been developed [52].

Although the effect of VEGF alone may be sufficient, literature recommends that the use of multiple growth factors in a synergistic manner would mimic natural conditions for tissue regeneration. Thus, bFGF, PDGF and EGF are often combined to VEGF in order to enhance tissue formation [51, 53-56].

For tissue engineering or drug delivery purposes, many studies suggest the use of growth factors as ELP-based conjugate. For example, apoptotic epidermal growth factor (EGF)-conjugated block copolymer micelles as a nanotechnology platform for targeted combination therapy has been developed (Figure 6) [57], construction of epidermal growth factor fusion proteins with cell adhesive and collagen binding activities for tissue repair and regeneration has also been designed fusing ELP and EGF covalently [46, 58]. The covalent fusion of elastin-like polypeptides with keratinocyte growth factor (KGF-ELP) formed nanoparticles for the treatment of chronic wounds [59].

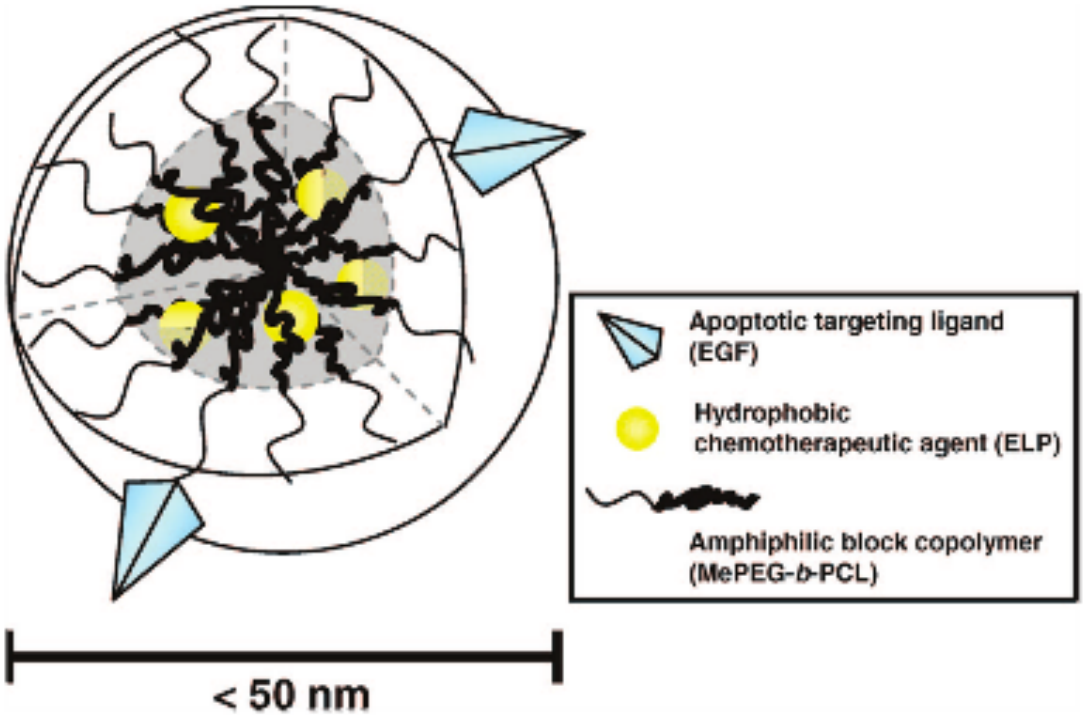

Figure 6: Schematic of Block copolymer micelles loaded with a chemotherapeutic agent in the hydrophobic core with apoptotic targeting ligand EGF conjugated to the hydrophilic shell [57].

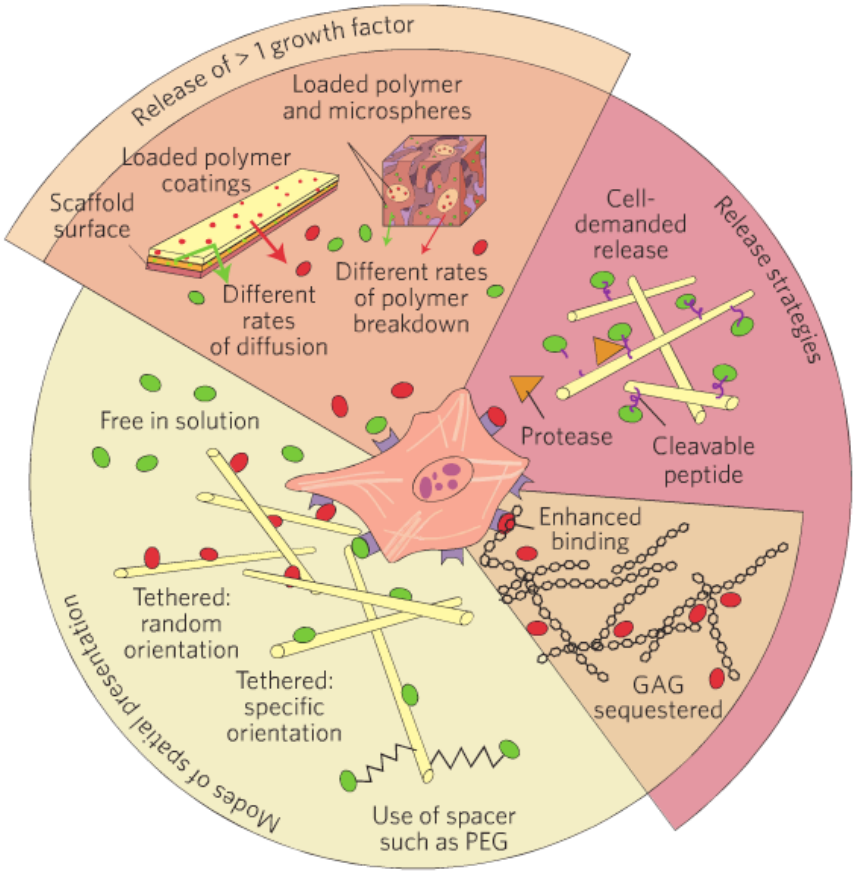

Figure 7: Presentation and release of growth factors from Tissue Engineered scaffolds. Anticlockwise, from top: growth factors within TE scaffolds may be loaded into polymers whose rate of degradation or diffusive properties can be modulated to tailor release rate, and which may be combined into systems releasing multiple factors with distinct kinetics. The exposure of cells to different growth factors with time may therefore imitate developmental pathways and healing responses. An alternative to presenting growth factors in soluble form is to bind them to a surface in either random or specific orientations, with the possible use of a spacer molecule. Non-covalent associations with matrix components, particularly glycosaminoglycans (GAGs), can effect slow release and in some cases may potentiate binding to membrane receptors. Cell-demanded release is based on the presence of protease-sensitive peptide sequences within the growth factor protein [60].

Developing tissue-engineered scaffolds or drug carriers along with immobilized growth factors for targeted application requires simplistic and consistent site-specific immobilization approach. Accordingly, protein-protein conjugation using covalent and non-covalent binding has been widely investigated (Figure 7) [60].

1.4 Protein-protein binding with coiled-coil

Ways of binding two or more proteins vary according to the nature of protein application. Covalent binding techniques have been frequently utilized. But, limitations using this technique showed to be inefficient.

Few studies reported potential drug delivery using non-covalent binding such as single walled carbon nanotubes for the transportation of small interferin RNAs [61], EGF tethered via coiled-coil interaction using Ecoil and Kcoil peptides to control cell adhesion, growth and differentiation [62], hybrid hydrogels assembled from synthetic polymers and coiled-coil protein domains (CC1 and CC2) [63] or coiled-coil peptide-based assembly of gold nanoparticles [64].

The discovery of coiled-coils goes back to Francis Crick and Pauling & Corey in 1952. Crick has described the packing of α-helices as simple coiled-coils. He suggested that the reason of deformation of coiled-coils was that the non-integer nature of the α-helix made it more likely that two helices having the same sense of twist would pack together at an angle rather than exactly parallel, and that this would lead to a coiled-coil. The energy to deform each helix into a curved helix or "coiled-coil" was shown to be very small [65]. Simultaneously Pauley & Corey have suggested that the origin of the deformation of coiled-coils is due to a repeating sequence of amino acids, a repeat every seventh residue being required for two-thirds of α-helices in the structure, and a repeat every fourth residue of two-ninths of them [66, 67]. Crick has also reported that the similarity between α-helix pattern and α-keratin pattern reflects the general type of structure, which it is believed to be α-helices arranged in a non-parallel manner for reasons of packing. It has also been shown that when α-helices of the same sense pack together, they will probably do so about 20 ° away from parallel and that for very long chains, it will lead to a coiled-coil [66].

Later, another kind of non-covalent binding has been profoundly studied that is the Fos, Jun and GCN4 leucine zippers. Fos and Jun oncogenes were found to associate *in vitro* due to the heptad repeat of leucine residues, which stabilizes the interaction between the Fos and Jun proteins. The transcription factors of bZIP class such as Fos, Jun and GCN4 regulate the expression of many different genes in organisms as diverse as fungi, plants and mammals (Figure 8) [68]. Studies of symthetic peptides have shown that leucine zipper short sequences are sufficient for dimerization of the GCN4 protein and for specific heterodimer formation by Fos and Jun. Leucine zippers are known to fold in a parallel coiled coils.

The coiled-coil motif has attracted continued attention as it is found in many proteins such as muscle proteins, α-keratin, bacterial surface proteins, intermediate filaments, laminin, dynein, tumor suppressors and oncogene products. Coiled coils also have been identified as ideal candidates for protein design. It has been reported that the coiled-coil structure consists of two right-handed α-helices wrapped around one another with a slight left-handed superhelical twist and the heptad repeats forming the coiled-coil proteins were labeled with letters **a-g**. Analysis of these sequences has shown that coiled-coil proteins have a characteristic 4-3 hydrophobic repeat, with hydrophobic amino acids spaced every four and then every three residues. The hydrophobic residues occur at positions **a** and **d** of the heptad repeat, whereas residues at positions **e** and **g** are predominantly charged.

O'Shea and colleagues developed two peptides, ACID-p1 and BASE-p1 which will be named in this study as helixA and helixB respectively [69]. These two peptides were designed following the Fos/Jun leucine zipper, which forms a favorable heterodimer formation under unfavorable interhelical electrostatic destabilization of the homodimer structure [70]. The difference between the coiled-coil formed by ACID-p1 and BASE-p1 and the leucine zipper is the **e** and **g** positions that have been replaced by glutamic acid in ACID-p1 and by lysine in BASE-p1 (Figure 9). Asparagine residue has been placed at **a** position in the second heptad to favor the parallel orientation of helices [69].

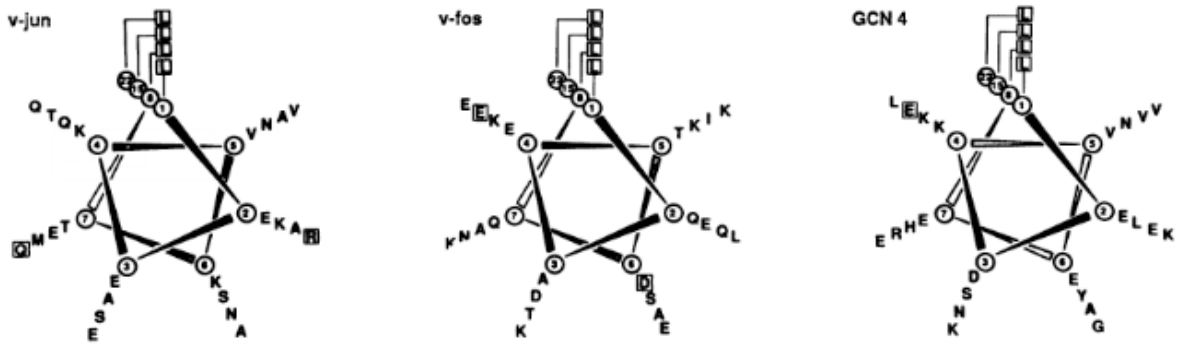

Figure 8: Conservation of leucine repeats between Fos, Jun and GCN4 [68].

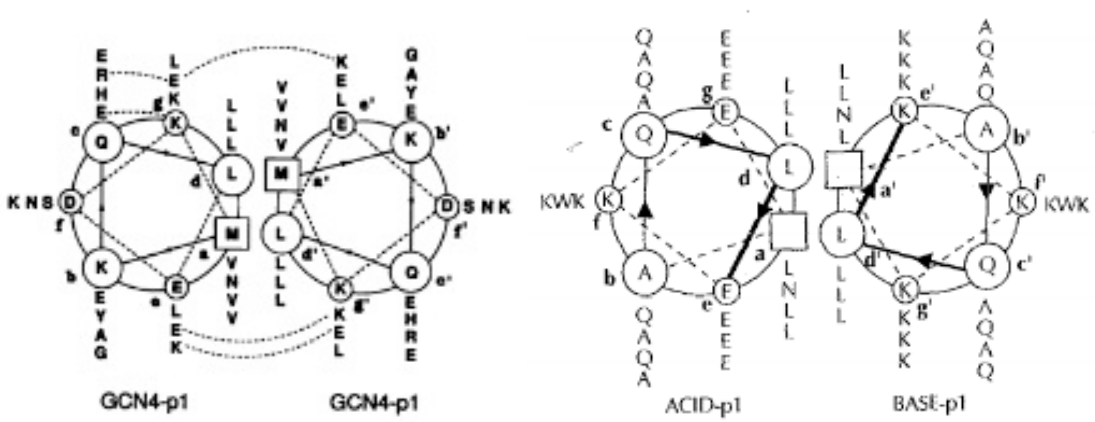

Figure 9: Helical wheel presentations of GCN4-p1, ACID-p1 and BASE-p1. The combination of two stranded and parallel coiled-coil GNC4-p1 is formed through the leucine zipper unlike the heterodimer formation between ACID-p1/BASE-p1 where coiled coils forms due to changes in **e** and **g** positions [69, 70].

1.5 Purpose of this study

Based on the approach cited in the previous section, this work aims at developing two different growth factor carriers involving elastin-like polypeptides using two α-helices ACID-p1 and BASE-p1 to form coiled coils. The detailed aims of this study are explained below:

- For tissue engineering, we describe the construction of coiled-coil structure used to maintain co-immobilized growth factors' activity on extracellular matrix for the promotion of angiogenesis in chapter 2.

- For drug delivery purposes, we describe the design of coiled-coil interaction between a growth factor and a thermo-responsive nanoparticle delivering paclitaxel drug to cancer cells in chapter 3.

This work focused on angiogenesis in health (tissue engineering) and disease (drug delivery). The formation of new blood vessels plays a significant role in tissue engineering and more importantly in wound repair process regulated by both angiogenic growth factors and extracellular matrix [71, 72]. Capillary blood vessels consist in endothelial cells that carry genetic information for tube-like formation [73]. These endothelial cells need a suitable ECM environment for cell migration, differentiation and development of new capillary-like tube structures.

Angiogenesis has often been associated to pathogenesis of some disorders such as tumorigenesis, psoriasis, arthritis or blindness when vessels grow excessively [71]. For that reason, many studies were focusing on inhibiting angiogenesis using the best-known inhibitor bevacizumab, which is a monoclonal antibody against vascular endothelial growth factor, as cancer treatment [74]. On the other hand, when abnormal and insufficient angiogenesis are arisen, other disorders are developed like heart and brain ischemia. To overcome this deficiency, protein and tissue engineering are required for therapeutic angiogenesis.

Therefore, this study would be valuable in broadways from extracellular matrix scaffolds to bio-grafts and from cell-sheets to nanoparticles.

1.6 References

[1] Gomes S, Leonor I, Mano J, Reis R, Kaplan D. Natural and Genetically Engineered Proteins for Tissue Engineering. Progress in polymer science 2012;37(1):1-17.

[2] Chan C, Berthiaume Fo, Nath B, Tilles A, Toner M, Yarmush M. Hepatic tissue engineering for adjunct and temporary liver support: critical technologies. Liver transplantation : official publication of the American Association for the Study of Liver Diseases and the International Liver Transplantation Society 2004;10(11):1331-42.

[3] Cortiella J, Nichols J, Kojima K, Bonassar L, Dargon P, Roy A, et al. Tissue-engineered lung: an in vivo and in vitro comparison of polyglycolic acid and pluronic F-127 hydrogel/somatic lung progenitor cell constructs to support tissue growth. Tissue engineering 2006;12(5):1213-25.

[4] Neumann T, Nicholson B, Sanders J. Tissue engineering of perfused microvessels. Microvascular research 2003;66(1):59-67.

[5] Hanjaya-Putra D, Wong KT, Hirotsu K, Khetan S, Burdick JA, Gerecht S. Spatial control of cell-mediated degradation to regulate vasculogenesis and angiogenesis in hyaluronan hydrogels. Biomaterials 2012;33(26):6123-31.

[6] Charriere G, Bejot M, Schnitzler L, Ville G, Hartmann DJ. Reactions to a bovine collagen implant. Clinical and immunologic study in 705 patients. Journal of the American Academy of Dermatology 1989;21(6):1203-8.

[7] Sakai D, Mochida J, Iwashina T, Watanabe T, Suyama K, Ando K, et al. Atelocollagen for culture of human nucleus pulposus cells forming nucleus pulposus-like tissue in vitro: influence on the proliferation and proteoglycan production of HNPSV-1 cells. Biomaterials 2006;27(3):346-53.

[8] Urry DW, Pattanaik A. Elastic protein-based materials in tissue reconstruction. Annals of the New York Academy of Sciences 1997;831:32-46.

[9] Dreher M, Simnick A, Fischer K, Smith R, Patel A, Schmidt M, et al. Temperature triggered self-assembly of polypeptides into multivalent spherical micelles. J Am Chem Soc 2008;130(2):687-94.

[10] Wright E, Conticello V. Self-assembly of block copolymers derived from elastin-mimetic polypeptide sequences. Advanced Drug Delivery Reviews 2002;54(8):1057-73.

[11] Wright E, McMillan R, Cooper A, Apkarian R, Conticello V. Thermoplastic Elastomer Hydrogels via Self-Assembly of an Elastin-Mimetic Triblock Polypeptide. Advanced functional materials 2002.

[12] Nagapudi K, Brinkman W, Leisen J, Thomas B, Wright E, Haller C, et al. Protein-Based Thermoplastic Elastomers. Macromolecules 2005.

[13] Martin L, Alonso M, Girotti A, Arias F, Rodriguez-Cabello J. Synthesis and characterization of macroporous thermosensitive hydrogels from recombinant elastin-like polymers. Biomacromolecules 2009;10(11):3015-22.

[14] Nagapudi K, Brinkman WT, Leisen JE, Huang L, McMillan RA, Apkarian RP, et al. Photomediated solid-state cross-linking of an elastin-mimetic recombinant protein polymer. Macromolecules 2002;35(5):1730-7.

[15] Nagapudi K, Brinkman W, Thomas B, Park J, Srinivasarao M, Wright E, et al. Viscoelastic and mechanical behavior of recombinant protein elastomers. Biomaterials 2005;26(23):4695-706.

[16] Kim W, Chaikof E. Recombinant elastin-mimetic biomaterials: Emerging applications in medicine. Advanced Drug Delivery Reviews 2010;62(15):1468-78.

[17] Fujita Y, Mie M, Kobatake E. Construction of nanoscale protein particle using temperature-sensitive elastin-like peptide and polyaspartic acid chain. Biomaterials 2009;30(2):3450-7.

[18] Herrero-Vanrell R, Rincon AC, Alonso M, Reboto V, Molina-Martinez IT, Rodriguez-Cabello JC. Self-assembled particles of an elastin-like polymer as vehicles for controlled drug release. Journal of controlled release : official journal of the Controlled Release Society 2005;102(1):113-22.

[19] Dreher M, Raucher D, Balu N, Michael Colvin O, Ludeman S, Chilkoti A. Evaluation of an elastin-like polypeptide-doxorubicin conjugate for cancer therapy. Journal of controlled release : official journal of the Controlled Release Society 2003;91(1-2):31-43.

[20] Betre H, Setton L, Meyer D, Chilkoti A. Characterization of a genetically engineered elastin-like polypeptide for cartilaginous tissue repair. Biomacromolecules 2002;3(5):910-6.

[21] Betre H, Ong S, Guilak F, Chilkoti A, Fermor B, Setton L. Chondrocytic differentiation of human adipose-derived adult stem cells in elastin-like polypeptide. Biomaterials 2006;27(1):91-9.

[22] McHale M, Setton L, Chilkoti A. Synthesis and in vitro evaluation of enzymatically cross-linked elastin-like polypeptide gels for cartilaginous tissue repair. Tissue engineering 2005;11(11-12):1768-79.

[23] Zio K, Tirrell D. Mechanical Properties of Artificial Protein Matrices Engineered for Control of Cell and Tissue Behavior. Macromolecules 2003.

[24] Heilshorn SC, DiZio KA, Welsh ER, Tirrell DA. Endothelial cell adhesion to the fibronectin CS5 domain in artificial extracellular matrix proteins. Biomaterials 2003;24(23):4245-52.

[25] Martinez-Osorio H, Juarez-Campo M, Diebold Y, Girotti A, Alonso M, Arias F, et al. Genetically engineered elastin-like polymer as a substratum to culture cells from the ocular surface. Current eye research 2009;34(1):48-56.

[26] Girotti A, Reguera J, Rodriguez-Cabello J, Arias F, Alonso M, Matestera A. Design and bioproduction of a recombinant multi(bio)functional elastin-like protein polymer containing cell adhesion sequences for tissue engineering purposes. Journal of materials science Materials in medicine 2004;15(4):479-84.

[27] Janorkar AV, Rajagopalan P, Yarmush ML, Megeed Z. The use of elastin-like polypeptide¬ñpolyelectrolyte complexes to control hepatocyte morphology and function< i> in vitro</i>. Biomaterials 2008;29(6):625-32.

[28] Swierczewska M, Hajicharalambous C, Janorkar A, Megeed Z, Yarmush M, Rajagopalan P. Cellular response to nanoscale elastin-like polypeptide polyelectrolyte multilayers. Acta biomaterialia 2008;4(4):827-37.

[29] Nakamura M, Mie M, Mihara H, Kobatake E. Construction of multi-functional extracellular matrix proteins that promote tube formation of endothelial cells. Biomaterials 2008;29(20):2977-86.

[30] Kobatake E, Onoda K, Yanagida Y, Haruyama T, Aizawa M. Design of a thermostable cell adhesion protein. Biotechnology Techniques 1999.

[31] Mie M, Mizushima Y, Kobatake E. Novel extracellular matrix for cell sheet recovery using genetically engineered elastin-like protein. Journal of biomedical materials research Part B, Applied biomaterials 2008;86(1):283-90.

[32] Meyer D, Kong G, Dewhirst M, Zalutsky M, Chilkoti A. Targeting a genetically engineered elastin-like polypeptide to solid tumors by local hyperthermia. Cancer research 2001;61(4):1548-54.

[33] McDaniel J, Callahan D, Chilkoti A. Drug delivery to solid tumors by elastin-like polypeptides. Advanced Drug Delivery Reviews 2010;62(15):1456-67.

[34] Betre H, Liu W, Zalutsky M, Chilkoti A, Kraus V, Setton L. A thermally responsive biopolymer for intra-articular drug delivery. Journal of controlled release : official journal of the Controlled Release Society 2006;115(2):175-82.

[35] Temenoff J, Mikos A. Injectable biodegradable materials for orthopedic tissue engineering. Biomaterials 2000.

[36] Hatefi A, Amsden B. Biodegradable injectable in situ forming drug delivery systems. Journal of controlled release : official journal of the Controlled Release Society 2002;80(1-3):9-28.

[37] Yu L, Ding J. Injectable hydrogels as unique biomedical materials. Chemical Society reviews 2008;37(8):1473-81.

[38] Adams S, Shamji M, Nettles D, Hwang P, Setton L. Sustained release of antibiotics from injectable and thermally responsive polypeptide depots. Journal of biomedical materials research Part B, Applied biomaterials 2009;90(1):67-74.

[39] Shamji MF, Whitlatch L, Friedman AH, Richardson WJ, Chilkoti A, Setton LA. An injectable and in situ-gelling biopolymer for sustained drug release following perineural administration. Spine 2008;33(7):748.

[40] Hart DS, Gehrke SH. Thermally associating polypeptides designed for drug delivery produced by genetically engineered cells. Journal of pharmaceutical sciences 2007;96(3):484-516.

[41] Zilberman M, Shifrovitch Y, Aviv M, Hershkovitz M. Structured drug-eluting bioresorbable films: microstructure and release profile. Journal of biomaterials applications 2009;23(5):385-406.

[42] Zilberman M, Eberhart RC. Drug-eluting bioresorbable stents for various applications. Annu Rev Biomed Eng 2006;8:153-80.

[43] Lao L, Venkatraman S. Paclitaxel release from single and double-layered poly(DL-lactide-co-glycolide)/poly(L-lactide) film for biodegradable coronary stent application. Journal of biomedical materials research Part A 2008;87(1):1-7.

[44] Kawatsu S, Oda K, Saiki Y, Tabata Y, Tabayashi K. External application of rapamycin-eluting film at anastomotic sites inhibits neointimal hyperplasia in a canine model. The Annals of thoracic surgery 2007;84(2):560-7.

[45] Kroll J, Waltenberger J. A novel function of VEGF receptor-2 (KDR): rapid release of nitric oxide in response to VEGF-A stimulation in endothelial cells. Biochemical and biophysical research communications 1999;265(3):636-9.

[46] Elloumi I, Kobayashi R, Funabashi H, Mie M, Kobatake E. Construction of epidermal growth factor fusion protein with cell adhesive activity. Biomaterials 2006;27(18):3451-8.

[47] Hori Y, Nakamura T, Kimura D, Kaino K, Kurokawa Y, Satomi S, et al. Effect of basic fibroblast growth factor on vascularization in esophagus tissue engineering. The International journal of artificial organs 2003;26(3):241-4.

[48] Whitaker MJ, Quirk RA, Howdle SM, Shakesheff KM. Growth factor release from tissue engineering scaffolds. The Journal of pharmacy and pharmacology 2001;53(11):1427-37.

[49] Nillesen ST, Geutjes PJ, Wismans R, Schalkwijk J, Daamen WF, van Kuppevelt TH. Increased angiogenesis in acellular scaffolds by combined release of FGF2 and VEGF. Journal of controlled release : official journal of the Controlled Release Society 2006;116(2):88-90.

[50] Backer M, Gaynutdinov T, Gorshkova I, Crouch R, Hu T, Aloise R, et al. Humanized docking system for assembly of targeting drug delivery complexes. Journal of controlled release : official journal of the Controlled Release Society 2003;89(3):499-511.

[51] De la Riva B, Sanchez E, Hernandez A, Reyes R, Tamimi F, Lopez-Cabarcos E, et al. Local controlled release of VEGF and PDGF from a combined brushite-chitosan system enhances bone regeneration. Journal of controlled release : official journal of the Controlled Release Society 2010;143(1):45-52.

[52] d'Angelo I, Garcia-Fuentes M, Parajo Y, Welle A, Vantus T, Horvath A, et al. Nanoparticles based on PLGA:poloxamer blends for the delivery of proangiogenic growth factors. Molecular pharmaceutics 2010;7(5):1724-33.

[53] Pepper MS, Ferrara N, Orci L, Montesano R. Potent synergism between vascular endothelial growth factor and basic fibroblast growth factor in the induction of angiogenesis in vitro. Biochemical and biophysical research communications 1992;189(2):824-31.

[54] Kim J, Jung Y, Kim S-H, Sun K, Choi J, Kim H, et al. The enhancement of mature vessel formation and cardiac function in infarcted hearts using dual growth factor delivery with self-assembling peptides. Biomaterials 2011;32(26):6080-8.

[55] Tarnawski A, Szabo I, Husain S, Soreghan B. Regeneration of gastric mucosa during ulcer healing is triggered by growth factors and signal transduction pathways. Journal of physiology, Paris 2001;95(1-6):337-44.

[56] Szabo S, Vincze A. Growth factors in ulcer healing: lessons from recent studies. Journal of physiology, Paris 2000;94(2):77-81.

[57] Lee H, Hu M, Reilly R, Allen C. Apoptotic epidermal growth factor (EGF)-conjugated block copolymer micelles as a nanotechnology platform for targeted combination therapy. Molecular pharmaceutics 2007;4(5):769-81.

[58] Hannachi Imen E, Nakamura M, Mie M, Kobatake E. Construction of multifunctional proteins for tissue engineering: epidermal growth factor with collagen binding and cell adhesive activities. Journal of biotechnology 2009;139(1):19-25.

[59] Koria P, Yagi H, Kitagawa Y, Megeed Z, Nahmias Y, Sheridan R, et al. Self-assembling elastin-like peptides growth factor chimeric nanoparticles for the treatment of chronic wounds. Proceedings of the National Academy of Sciences of the United States of America 2011;108(3):1034-9.

[60] Place E, Evans N, Stevens M. Complexity in biomaterials for tissue engineering. Nature materials 2009;8(6):457-70.

[61] Krajcik R, Jung A, Hirsch A, Neuhuber W, Zolk O. Functionalization of carbon nanotubes enables non-covalent binding and intracellular delivery of small interfering RNA for efficient knock-down of genes. Biochemical and biophysical research communications 2008;369(2):595-602.

[62] Boucher C, Ruiz JC, Thibault M, Buschmann MD, Wertheimer MR, Jolicoeur M, et al. Human corneal epithelial cell response to epidermal growth factor tethered via coiled-coil interactions. Biomaterials 2010;31(27):7021-31.

[63] Wang C, Stewart R, Kopecek J. Hybrid hydrogels assembled from synthetic polymers and coiled-coil protein domains. Nature 1999;397(6718):417-20.

[64] Stevens MM, Flyn NT, Wang C, Tirrell DA, Langer R. Coiled-Coil Peptide-Based Assembly of Gold Nanoparticles. Advanced Materials 2004;16.

[65] Crick F. Is alpha-keratin a coiled coil? Nature 1952;170(4334):882-3.

[66] Crick F. The packing of α-helices: simple coiled-coils. Acta Crystallographica 1953.

[67] Pauling L, Corey R. Compound helical configurations of polypeptide chains: structure of proteins of the alpha-keratin type. Nature 1953;171(4341):59-61.

[68] Landschulz W, Johnson P, McKnight S. The leucine zipper: a hypothetical structure common to a new class of DNA binding proteins. Science (New York, NY) 1988;240(4860):1759-64.

[69] O'Shea EK, Lumb KJ, Kim PS. Peptide 'Velcro': design of a heterodimeric coiled coil. Current biology : CB 1993;3(10):658-67.

[70] O'Shea EK, Rutkowski R, Stafford WF, 3rd, Kim PS. Preferential heterodimer formation by isolated leucine zippers from fos and jun. Science 1989;245(4918):646-8.

[71] Carmeliet P. Angiogenesis in health and disease. Nature medicine 2003;9(6):653-60.

[72] Li J, Zhang YP, Kirsner RS. Angiogenesis in wound repair: angiogenic growth factors and the extracellular matrix. Microscopy research and technique 2003;60(1):107-14.

[73] Folkman J, Shing Y. Angiogenesis. The Journal of biological chemistry 1992;267(16):10931-4.

[74] Shih T, Lindley C. Bevacizumab: an angiogenesis inhibitor for the treatment of solid malignancies. Clinical therapeutics 2006;28(11):1779-802.

Chapter 2

The promotion of angiogenesis by growth factors integrated with ECM proteins through coiled-coil structures

---

"Anybody who has been seriously engaged in scientific work of any kind realizes that over the entrance to the gates of the temple of science are written the words: 'Ye must have faith'." – Max Plank

2.1. Introduction

Angiogenesis, formation of new blood vessels, plays a significant role in tissue engineering and more importantly in wound repair process regulated by both angiogenic growth factors and extracellular matrix (ECM) [1, 2]. Capillary blood vessels consist in endothelial cells (EC) that carry genetic information for tube-like formation [3]. These ECs need a suitable ECM environment for cell migration, differentiation and development of new capillary-like tube structures.

The ECM elements such as fibronectin, collagen, elastin and laminin are required to preserve healthy ECs growth and organization. We, therefore, previously constructed an artificial ECM designated as EREI2 [4], which consisted in two repeats of 12 repetitive sequence of polyhexapeptides $(APGVGV)_{12}$, RGD peptide and IKVAV sequence. Repetitive sequence of APGVGV, an elastin-like polypeptide, reported to form a stable spiral structure that easily attaches onto hydrophobic surfaces and possesses cell-adhesive properties [5, 6]. The arginine-glycine-aspartic acid (RGD) peptide known to be a biodegradable material, promotes cell-adhesion [7, 8] and IKVAV sequence, a laminin derived pentapeptide also promoting cell-adhesion, differentiation and migration [9], interacts with endothelial cells, plays an important role in cell recognition and induces angiogenic behaviour [10, 11].

Besides, to preserve a constant delivery of the artificial ECM, we used atelocollagen, a digested collagen, to prolong retention of the fusion protein. Atelocollagen has been clinically used as skin disorder treatment [12] due to its low antigenecity by removing the antigenic telopeptide region using pepsin digestion. Atelocollagen proved to be a safe scaffold as a treatment in tissue engineering and cell transplantation [13]. In order to bind EREI2 to atelocollagen, human fibronectin-derived collagen-binding domain (CBD) [14] was used as a fusion partner of EREI2.

In addition to ECM, appropriate growth factors such as $VEGF_{121}$, commonly known in angiogenesis activation, are needed to develop a proper environment for cell sprouting and tubular network formation. Ways of linking growth factors to ECM proteins have been extensively discussed. Previously, direct linking between ECM and GF was used by

direct fusion. However, some disadvantages have been reported like biological activity loss or adsorption limitations of cell adhesion [15].

Thus, fusing proteins non-covalently seems to retain their activity and may be a methodology to overcome problems encountered with using covalent binding [16]. In our previous study, bFGF was tethered to ECM non-covalently [17]. The non-covalent model we used in that study relies on O'Shea and colleagues who developed two peptides, ACID-p1 (helixA) and BASE-p1 (helixB) [18]. These two peptides were designed following the Fos/Jun leucine zipper, which forms a favorable heterodimer formation under unfavorable interhelical electrostatic destabilization of the homodimer structure [19].

In this study, we have developed a fusion protein (CBDEREI2-helixB) corresponding to CBDEREI2 fused at its C-terminus to helixB. In order to promote the interaction of the helixB peptide moiety with its interacting peptide partner helixA, helix A was fused with growth factor at its N-terminal. It has been reported that using both basic fibroblast growth factor (bFGF) and VEGF at the same time increased angiogenesis and blood vessel maturation [20, 21]. Additionally, epidermal growth factor (EGF) is a pro-angiogenic growth factor. Hence, we decided to amplify the signal transduction and the synergistic effect by co-immobilizing single-chain $VEGF_{121}$, bFGF and EGF each fused with helixA at their N-terminal to form helixA-sc$VEGF_{121}$, helixA-bFGF and helixA-EGF respectively (Fig. 1).

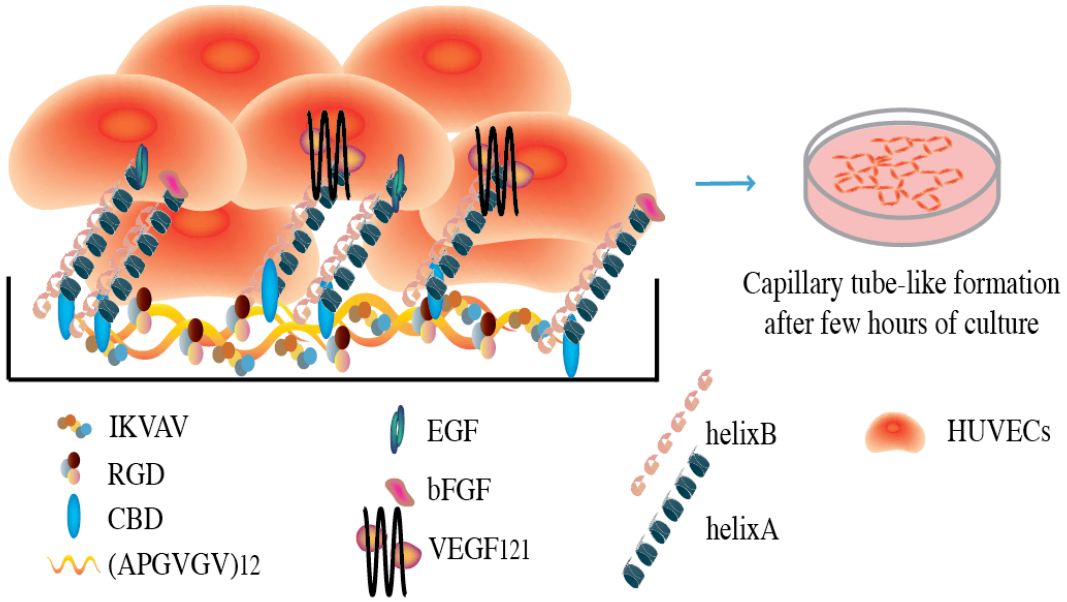

Figure 1: Schematic illustration of non-covalent binding of the designed ECM to multi-growth factors through coiled-coil structure to promote angiogenesis.

2.2. Materials and methods

2.2.1. Plasmid Construction

Four plasmids were constructed to conduct the experiments described in this paper: pET-helixA-scVEGF$_{121}$, pET32c-helixA-bFGF, pET32c-helixA-EGF and pET-CBDEREI2-helixB. To obtain VEGF$_{121}$ gene, Reverse transcription (RT) was performed with HUVEC mRNA using Superscript III First-Strand Synthesis System (Invitrogen, Carlsbad, CA) primed by Oligo-dT for cDNA synthesis. VEGF$_{121}$ was amplified by PCR with VEGF (forward) and VEGF (reverse) primers introducing *Eco*RI at the 5' and *Hind*III at the 3'. The obtained fragment was inserted in pUC18 vector. pUC18-VEGF was confirmed by sequencing. To compensate the frameshift treatment occurred after the *Bam*HI site, the sequence was digested with *Bam*HI followed by Mung Bean nuclease treatment (Takara). A linker fragment was introduced in pUC18 using *Eco*RI and *Nco*I enzymes after annealing with linker fragment 1 and linker fragment 2. The new fragment was digested and inserted into the pUC18- VEGF$_{121}$ with *Bam*HI and *Hind*III enzymes. The resulting plasmid was named pUC18-scVEGF$_{121}$. VEGF$_{121}$-linker-VEGF$_{121}$ was digested with *Nco*I and *Hind*III and inserted with the same enzyme into the pET-His(*Nco*I) [22]. The resulting plasmid was named pET-His(*Nco*I)-scVEGF$_{121}$. Helix A of pET-32c-helixA-bFGF, constructed as described previously [17], was amplified using a pair of primer containing *Eco*RI restriction sites and was inserted in pUC18-scVEGF$_{121}$. His-helixA-scVEGF$_{121}$ was then inserted into pET-His(*Nco*I) after removal of His fragment. The resulting plasmid was designated as pET-His(*Nco*I)-helixA-scVEGF$_{121}$. EGF fragment was cut using *Bam*HI and *Hind*III from pBS-EGF [23] and inserted into pBS-helixA. HelixA-EGF was digested and inserted with the same enzyme into pET32c vector. The obtained plasmid is referred as pET32c-helixA-EGF. HelixB in pET-ERE-helixB [17] was amplified using a pair of primer containing *Bam*HI and *Pst*I restriction sites and was inserted in pET32c-EREI2. The obtained plasmid was digested and inserted in pET32c-NHis-fnCBD [4] using *Bam*HI and *Hind*III to get pET32c-NHis-CBDEREI2-helixB (Fig. 2A). All primers used in this experiment see Table 1.

Table 1: primers used for plasmid construction.

VEGF	
Forward primer (5' – 3')	GGCGAATTCCCCCATGgcaccGatggcagaaggaggaggg
Reverse primer (5' – 3')	GGCCAAGCT-TtcaccgGATCcctcggcttgtcacatttttc
Linker fragment 1	CATGcCTTTGCCTTCCGATTTGCCAGAGCC-GGAGGTGGATCcAATT
Linker fragment 2	gGATCCACCTCCGGCTCTGGCAAATCCTCGGAAGGCAA-AGGC
helixA	
Forward primer (5' – 3')	cgcgaattcTTGAGCGAGCTCTTTCTCCAG
Reverse primer (5' – 3')	gttttgcgGAattcgatggt
helixB	
Forward primer (5' – 3')	tggcaccaaGGATCCgcggtggatc
Reverse primer (5' – 3')	AGTTTGCGCAACGTTGTTGC

Table 2: Primers for gene expression

Gene analyzed	Forward primer (5' – 3')	Reverse primer (5' – 3')	Annealing temp. (°C)
Ang-2	aaagactgggaagggaatgagg	gatgtttagaaatctgctggtcgg	62
Tie-2	ggatacgaaccatgaagatgcg	ccaaacgtgtgcagttcacaag	62
MMP-2	gtgctgaaggacacactaaagaaga	ttgccatccttctcaaagttgtagg	62
GAPDH	*278:* ccatcaccatcttccaggag	*853:* cctgcttcaccaccttcttg	62

2.2.2. Expression and purification of fusion protein

pET-helixA-scVEGF121 and pET32c-CBDEREI2-helixB plasmids were transfected into *E.coli* BL21(DE3) competent cells and pET32c-helixA-EGF and pET32c-helixA-bFGF into *E.coli* KRX competent cells by heat shock and cultured at 37 °C in a Luria-Bertani (LB) medium supplemented with ampicillin to an optical density of 0.6 at 600 nm. Protein expression was induced by addition of 1 mM isopropylthio-ß-D-galactoside (IPTG) only for pET-helixA-scVEGF121 and pET32c-CBDEREI2-helixB. In addition of IPTG, 0.1% rhamnose was added to pET32c-helixA-EGF and pET32c-helixA-bFGF for protein induction. Cells were cultured at 30 °C for 4 h, harvested by centrifugation (8 000 g) and resuspended in Bug Buster Reagent and Benzonase nuclease followed by rotation at room temperature for 30 min before repelleting by centrifugation (8 000 g) for 10 min. ***Protein extraction from soluble fraction***: The supernatant was collected and purified by His select TALON Metal Affinity Resins (Clontech) using a Poly prep column (Bio-Rad). After 30 min incubation at 4 °C, the column was washed three times with four-column volumes of the wash buffer (50 mM sodium phosphate, 300 mM NaCl, pH 7.6) and followed by three times with four volumes of the same buffer including 5 and 10 mM imidazole each. The fusion proteins were eluted with two-column volume of elution buffer (50 mM sodium phosphate, 300 mM NaCl, 100 mM imidazole, pH 7.6). The fusion proteins were then dialyzed in a PBS buffer overnight using a Slider-A-lyzer dialysis cassette (PIERCE). ***Protein extraction from inclusion bodies***: The supernatant was discarded and the proteins were extracted from the inclusion bodies for pET-helixA-scVEGF121 and pET32c-CBDEREI2-helixB and solubilised with 8M Urea PBS for overnight at 4 °C. The supernatant was collected by centrifugation (8 000 g) for 10 min and purified by His select TALON Metal Affinity Resins (Clontech) using a Poly prep column (Bio-Rad). After 30 min incubation at 4 °C, the column was washed three times with four-column volumes of the wash buffer (50 mM sodium phosphate, 300 mM NaCl, 4 M Urea, pH 7.6) and followed by three times with four volumes of the same buffer including 5 and 10 mM imidazole each. The fusion proteins were eluted with two-column volume of elution buffer (50 mM sodium phosphate, 300 mM NaCl, 4 M Urea, 100 mM imidazole, pH 7.6). The fusion proteins were then dialyzed against serial dilutions of urea

(2 M, 1 M and 0.5 M Urea) and PBS only with one hour each and finally against PBS buffer overnight using a Slider-A-lyzer dialysis cassette (PIERCE). The purity of the proteins was analyzed by 12 % sodium dodecyl sulfate polyacrylamide gel electrophoresis (SDS-PAGE) and the concentration was determined using a BCA assay kit (PIERCE).

2.2.3. Evaluation of protein binding through coiled-coil structure

To show the specific binding between helixA and helixB as well as the optimum concentration of our fusion proteins to be used in further experiments, 96-well ELISA plates (Costar 3361, Corning Life sciences, Lowel, MA), were coated for 3 h at 37 °C with 100 nM of CBDEREI2-HelixB. Plates were washed 3 times with PBS-T and blocked overnight with 2 % bovine serum albumin (BSA) in PBS buffer at 4 °C. After blocking, plates were washed again and incubated with helixA-scVEGF$_{121}$, helixA-bFGF and helixA-EGF separately at different concentrations each (1 nM, 10 nM, 100 nM and 1 μM) for 2 h at 37 °C. After washing, anti-VEGF$_{121}$ (Abcam Life Sciences, Cambridge, MA), anti-bFGF and anti-EGF (Sigma-Aldrich) antibodies were reacted for 1 h at 37 °C. HRP-conjugated secondary IgG at 1:1000 dilution were added and reacted for 1 h at 37 °C. TMB peroxidase substrate (KPL, Gaithersburg, MD) was added after washing three times with PBS-T and reaction was stopped after 5 min by adding 1 N HCl. The binding was detected and measured spectrophotometrically at a wavelength of 450 nm (Benchmark, Bio-Rad).

2.2.4. Evaluation of cell-adhesive activity of CBDEREI2-HB

Cell adhesion assays were performed in a 24-well non-tissue culture plate (Sumilon MS-8024R, Japan). The surface of the wells was coated with 100 nM of CBDEREI2-helixB, 100 nM of fnCBD, fibronectin and 1% BSA respectively. Fibronectin (Sigma-Aldrich) was added at a concentration of 10 μg/ml and was used as a positive control. 1% BSA coated surfaces and non-coated surfaces were used as negative control. After incubation for 1 h at 37 °C, wells were washed three times with PBS-T and blocked with 1% BSA in PBS buffer overnight at 4 °C. (HUVECs) (Kurabo Industries, Japan) cultured

in growth medium HuMedia-EG2 (Kurabo Industries, Japan) supplemented with 2% FBS, 10 μg/l hEGF, 5 mg/l hFGF-B, 10 mg/l heparin, 1 mg/l hydrocortisone, 50 mg/l gentamicin, 50 μg/l amphotericin B, were seeded at a density of $6x10^4$ cells/well. After 4 h incubation at 37 °C, wells were washed three times with PBS-T. The remaining number of attached cells on the plate was examined by cell counting kit (CCK8-kit, Dojindo, Japan) and the absorbance was measured in a micro plate reader at a wavelength of 450 nm (Benchmark, Bio-Rad). Each sample was assayed in triplicate wells. Confluent HUVECs (passages 4~7) were used for the experiments.

2.2.5. Collagen-binding activity of CBDEREI2-HB

Ninety-six well ELISA plates were coated for 1 h at 37 °C with either pepsin-solubilized type I collagen (Atelocollagen I PC-30, Koken, Japan) at 3 mg/ml, pH 3.0 or acid-solubilized type I collagen (Native collagen I AC-30, Koken, Japan) at 3 mg/ml, pH 3.0 or BSA at 1%. Plates were washed 3 times with PBS-T and non-specific binding was blocked by overnight incubation with 1% BSA in PBS buffer at 4 °C. After blocking, plates were washed again and incubated with increased concentration of CBDEREI2-helixB (100 nM, 500 nM and 1 μM) at 37 °C for 1 h. After washing, plates were incubated with anti-His-Tag antibody (Sigma-Aldrich). Bound antibodies were detected as previously mentioned in evaluation of protein binding through coiled-coil structure.

2.2.6. Cell proliferative activity of growth factor with helixA

HUVECs were suspended in HuMedia-EG2 then seeded in 24-well tissue culture plates (Falcon, BD Bioscience) at a density of 5×10^3 cells/well. After 1 day of culture, purified fusion proteins (helixA- $scVEGF_{121}$, helixA-bFGF, helixA-EGF) were added with increased concentrations (1 nM, 10 nM and 100 nM) and purchased wild-type $VEGF_{121}$ (10 nM of rhVEGF- A_{121}) (Wako Chemicals, Japan), 10 nM hEGF and 10 nM hFGF-B (Kurabo, Japan) were used as positive control. The day on which proteins were added was defined as day 0. The activity was evaluated at 450 nm as mentioned in the Cell Counting Kit (CCK-8) every 2 days until day 7.

2.2.7. Growth factor activity of adsorbed helixA-scVEGF121

CBDEREI2-helixB was mixed with helixA- scVEGF121 and incubated at 37 °C for 1 h on a shaker. 24-well non-tissue culture plate was coated by the coiled-coil structure formed after incubation and allowed to attach to the plate at 37 °C for 1 h. Wells were washed by PBS then HUVECs were seeded onto coated plates and the remaining attached cells were counted as described in the previous section. The attached cells' growth kinetics was followed for 4 days. Day 0 of the kinetics was the day on which the incubation of the remaining attached cells was started. The medium was changed every 2 days.

2.2.8. Tubulogenesis promoting activity in collagen culture

Collagen type I gel medium was prepared as recommended by Koken Industries as follows: 3 mg/ml atelocollagen type I (Koken, I-PC, Japan) was mixed with 5xPBS buffer in a volume ratio of 1:5, 1 M Hepes buffer (final concentration, 10 mM) and 1 M $NaHCO_3$ in a volume ratio of 1:100. The medium was stored at 4 °C until use. Before mixing gel-medium and fusion proteins, different combinations of coiled-coil structures were prepared.

1 μM of each fusion protein was added into 1.5 ml microtube. Fusion proteins were incubated at 37 °C for 1 h to form complex between helixA and helixB. 1:3 volume of protein combinations was added to the collagen gel-medium. The prepared atelocollagen-protein gel mix was added to a 6-well tissue culture plate (Falcon, BD Bioscience) and allowed to gel at 37 °C for 2 h.

HUVECs were seeded onto the gel surfaces at the density of 3 x 10^5 cells/well and incubated at 37 °C for 1 h for cell attachment. Non-attached cells were removed by pipetting and HuMedia-EG2 without growth factors was supplied to the wells. The well containing atelocollagen only coated with HUVECs and supplied with HuMedia-EG2 without growth factors was used as negative control. The well containing atelocollagen only coated with HUVECs and supplied with HuMedia-EG2 with commercialized growth factors was defined as positive control. The morphology of HUVECs atelocollagen-protein

gel mix was monitored and photographed with a phase contrast microscope (Olympus, Japan).

2.2.9. Gene expression

HUVECs were cultured as mentioned in the previous section. After 4 days of culture, Atelollagen-protein gel mix was degraded with 0.1 % collagenase (Nitta gelatine, Japan) for 45 min at 37 °C on a shaking incubator to recover cells. Total RNA was isolated using TRIzol reagent (Invitrogen, Carlsbad, CA). RT was performed using the Superscript III First-Strand Synthesis System primed by Oligo-dT. First-strand complementary DNA (cDNA) was then amplified by polymerase chain reaction (PCR) using the primers shown in Table 2. The reaction mixtures (12 μl) were subjected to the following cycling conditions: initial denaturation for 4 min at 94 °C; 30 or 40 cycles of denaturation for 30 s at 94 °C, annealing for 1 min at 62 °C and extension for 1 min at 72 °C. the amplified DNAs were analyzed by 1.5 % agarose gel electrophoresis with ethibium bromide staining.

2.3. Results

2.3.1. Expression of fusion proteins

In our previous study, CBDEREI2 containing two repeats of elastin-derived unit $(APGVGV)_{12}$, cell-adhesive sequence (RGD) and laminin-derived IKVAV sequence fused with collagen-binding domain (CBD) was engineered to obtain CBDEREI2. We fused this fragment with helixB, which in turn was fused with helixA to coiled-coil formation with growth factor proteins. The designed fusion proteins were either expressed in *E.coli* BL21(DE3) or KRX strains. To facilitate the purification, based on a one-step immobilized metal affinity chromatography (IMAC) resin, a hexahistidine tag was introduced at the N-terminus of the fusion proteins expressed in BL21 (DE3). For those expressed in KRX, thioredoxin was additionally introduced between the N-terminus and the hexahistidine tag to increase solubility (Fig. 2A). CBDEREI2-helixB and helixA- $scVEGF_{121}$ were purified from the insoluble fraction using the TALON metal affinity resin. HelixA-EGF and helixA-bFGF were purified from the soluble fraction also using the TALON metal affinity resin. Thioredoxin was removed using an enterokinase cleavage capture kit (Novagen, EMD Bioscience, Germany). The purity of the fusion proteins was analyzed with 12 % SDS-PAGE. The results validated the expected size ranges: CBDEREI2-helixB (60.5 kDa), helixA- $scVEGF_{121}$ (34.3 kDa), helixA-bFGF (21 kDa), helixA-EGF (11.4 kDa) (Fig. 2B). The experimental results are consistent with the calculated molecular masses. The fusion proteins were purified enough for further experiment, as indicated by SDS-PAGE.

2.3.2. Protein binding through coiled-coil structure

ELISA analysis was performed to examine the binding ability of helixA to helixB (Fig. 3A). Anti-VEGF, anti-FGF2 and anti-EGF antibodies were used and the signals were detected with HRP-conjugated secondary antibodies. The results (Fig. 3B) showed that signal increased in a dose dependent manner up to 1 μM and demonstrated that 10 nM of fusion proteins are enough to trigger the complex formation of helixA and helixB. Furthermore, these results established that the non-covalent binding formed through coiled-coiled structure could function as an effective bridge connecting growth factor

fusion proteins and extracellular matrix protein. On the basis of these results, we optimized the concentration of fusion proteins to be used for further experiments.

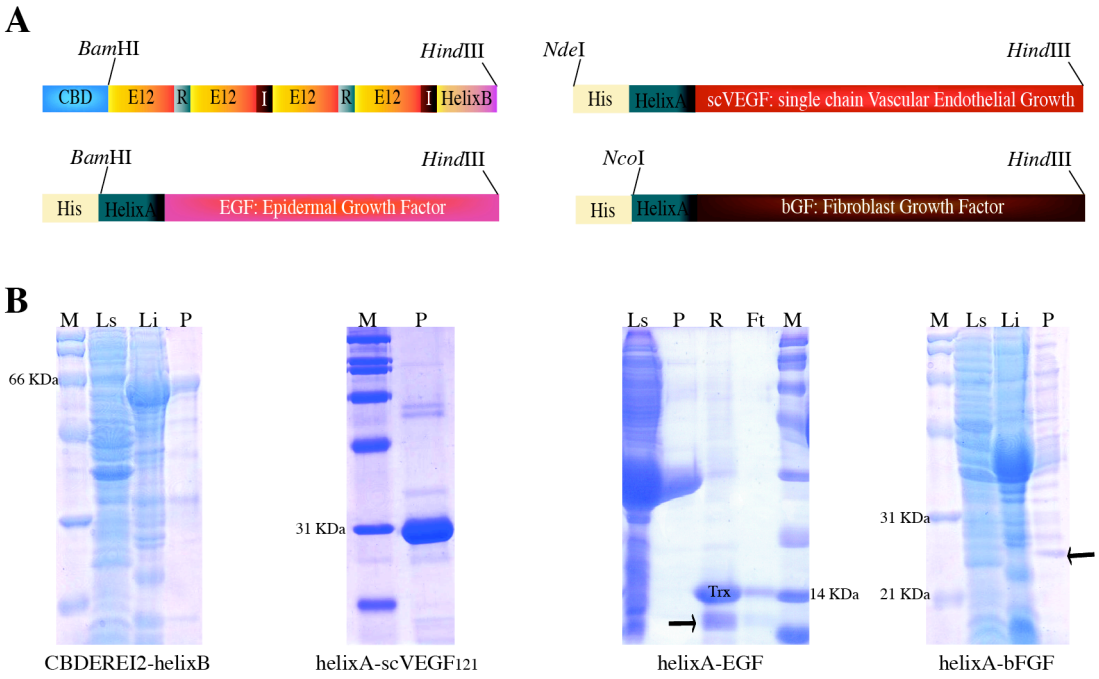

Figure 2: Expression and purification of CBDEREI2-helixB, helixA-scVEGF121, helixA-EGF and helixA-bFGF. (A) Constructed plasmids pET32c-NHis-CBDEREI2-helixB, pET-NHis-helixA- scVEGF121, pET32c-helixA-EGF and pET32c-helixA-bFGF. Fused fragments were cloned into pET-NHis and pET32c backbone under the regulation of T7 promoter. Histidine tag sequence (His-tag) was used upstream for purification of the recombinant protein. (B) SDS-PAGE of constructed proteins respectively CBDEREI2-helixB, helixA- scVEGF121, helixA-EGF and helixA-bFGF. Legend: M: marker; Ls: lysate from soluble fraction; Li: lysate from insoluble fraction; P: purified protein; R: Talon resin; Ft: flow through after thioredoxin cut.

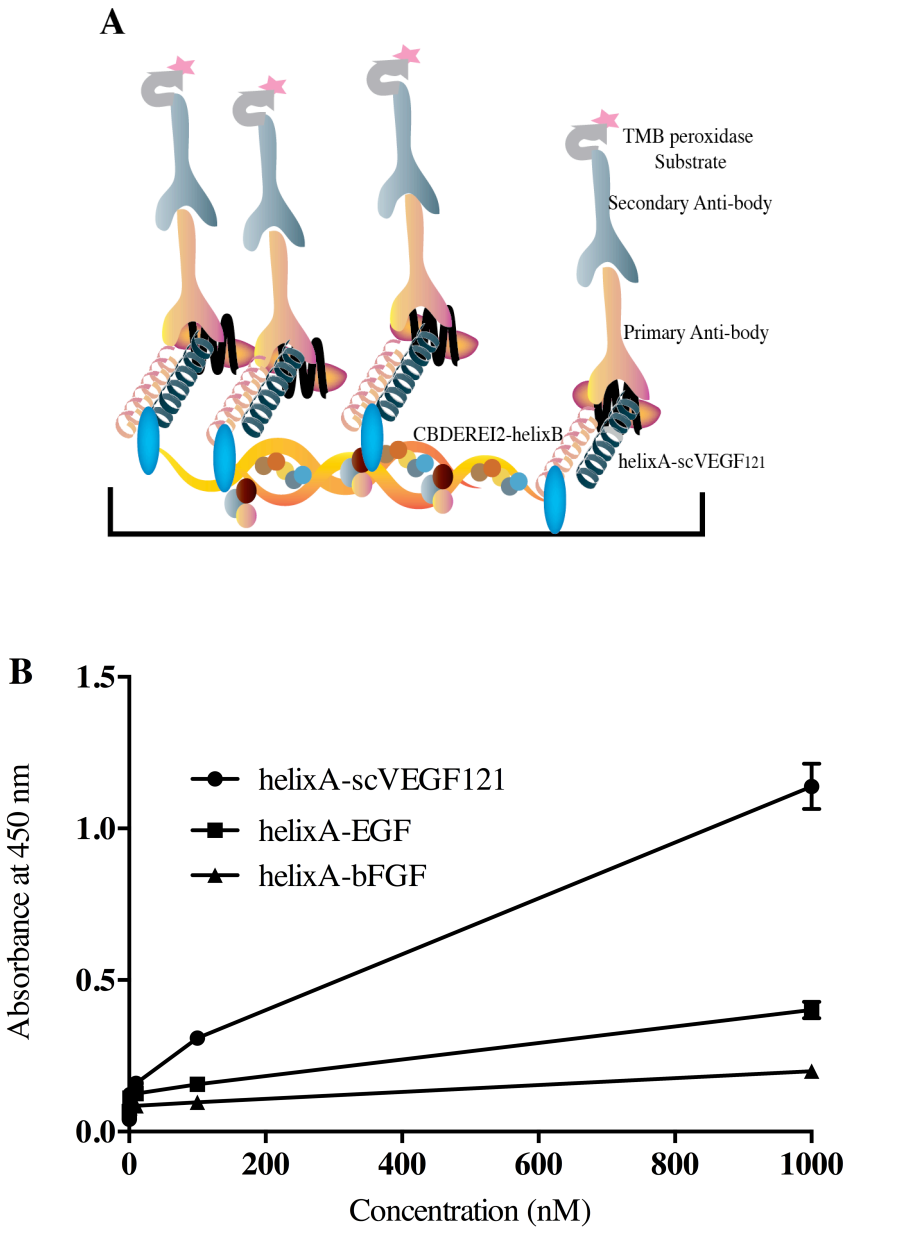

Figure 3: Binding of helixA-scVEGF121, helixA-EGF and helixA-bFGF to CBDEREI2-helixB through coiled-coil structure on ELISA plate. (A) Experimental scheme used for ELISA. (B) Various concentrations of helixA-scVEGF121, helixA-EGF and helixA-bFGF were reacted with CBDEREI2-helixB adsorbed onto 96-well plate surface. The amounts of bound helixA-scVEGF121, helixA-EGF and helixA-bFGF were evaluated after HRP IgG binding.

2.3.3. Collagen binding affinity of CBDEREI2-helixB

The collagen-binding property of the fusion protein was essayed. Native collagen and atelocollagen were coated on the plate before adding different concentrations of CBDEREI2-helixB. Figs. 4A and B shows that CBDEREI2-helixB specifically bound to collagen in a dose-dependent manner, whereas it did not bind to blocking proteins that was considered as nonspecific binding. CBDEREI2-helixB showed a significantly higher affinity to atelocollagen up to twice than to native collagen. In contrast, low binding of fnCBD was observed in both native collagen and atelocollagen. These results indicated that CBDEREI2-helixB has the property to bind to a biomaterial with low antigenicity and high bioaffinity and demonstrated that EREI2-helixB moiety plays a pivotal role in enhancing the binding affinity. Based on these findings, atelocollagen was selected for further studies.

2.3.4. Adhesion of cells on designed extracellular matrix

For the establishment of CBDEREI2-helixB as a fusion protein-based ECM, adhesion efficiency of HUVECs on CBDEREI2-helixB, fnCBD, fibronectin and 1% BSA was evaluated. Fibronectin and BSA were used as positive and negative control, respectively. Results showed HUVECs adhered to the CBDEREI2-helixB-coated surface with almost the same potency as to the conventional fibronectin-coated surface whereas CBDEREI2-helixB matrix showed better cell adhesion than on fnCBD (Fig. 5). These findings prove the importance of fusing EREI2-helixB to CBD as EREI2-helixB contains RGD sequence responsible for cell-adhesion. It also encourages our hypothesis that CBDEREI2-helixB may stimulate endothelial cell proliferation.

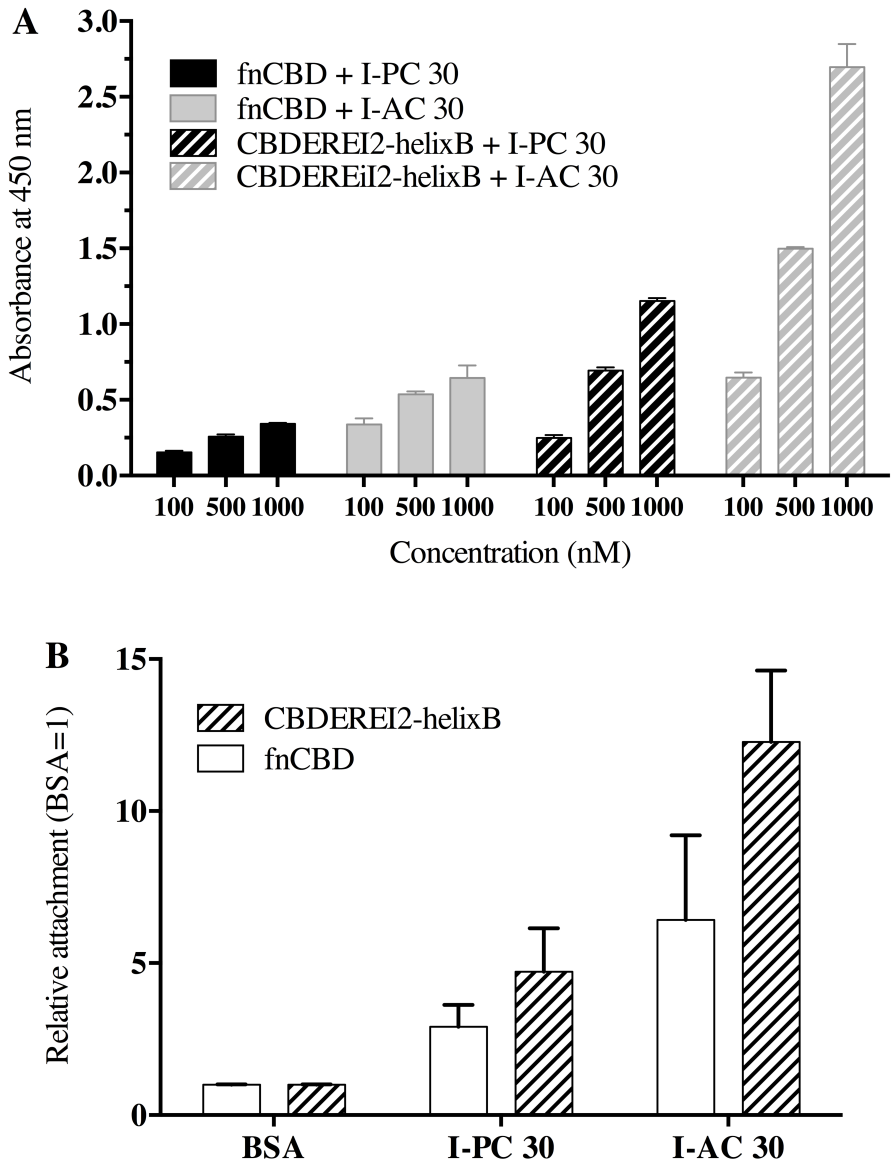

Figure 4: Collagen binding characteristics of the CBDEREI2-helixB. (A) Binding to Native collagen (I-PC 30) or atelocollagen (I-AC 30) coated plate surface. 96 well-plate were coated with either I-PC 30 or I-AC 30. FnCBD and CBDEREI2-helixB were added to the wells at different concentrations. Binding properties of the CBDEREI2-helixB was confirmed with ELISA using anti-His-tag antibody. (B) Relative attachment to 1% BSA of 1 μM of fnCBD and 1 μM of CBDEREI2-helixB on both I-PC 30 and I-AC 30.

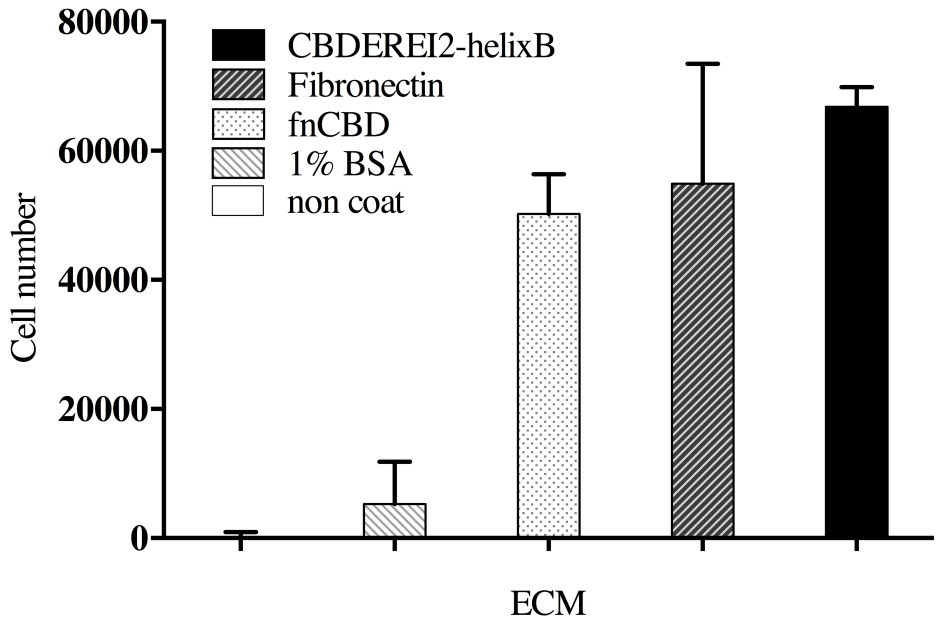

Figure 5: Cell-adhesive activity of CBDEREI2-helixB. 100 nM of CBDEREI2-helixB, 100 nM of fnCBD, 10 μg/ml fibronectin and 1% BSA were added to each well of 24-well non-tissue culture plate. HUVECs were seeded to the coated wells and the number of adhesive cells after 4 h incubation was counted. The positive control was fibronectin.

2.3.5. Induction of cell proliferation by helix fused scVEGF121

Cell growth-promoting activity of helixA-scVEGF121 in the free form was examined using HUVECs monolayer cell culture condition. Fig. 6A shows that the dose-response curves of helixA-scVEGF121, helixA-bFGF and helixA-EGF (data not shown) were similar to that of the wild-type versions of the above mentioned growth factors. The fusion proteins induced cell growth on day 5 with only 1 nM of helixA-scVEGF121 while 10 nM of wild-type VEGF121 was needed to obtain comparable results. This confirmed the activity and cell growth-promoting capabilities of helixA- scVEGF121. The weak absorbance signal of cells in medium without growth factor corresponds to the slow growth of HUVECs (Fig. 6B). This suggests that the increase of absorbance is correlated with the presence of our fusion proteins. To determine the sustainability of the release period of the active growth factor fusion proteins bound to CBDEREI2-helixB, HUVEC cells were seeded onto plates previously coated with fused extracellular matrix and fused growth factors with medium change every 2 days. As a control, we seeded HUVECs on a non-coated plate. In both cases, cells were supplied in medium without growth factor. Our results showed that there was no proliferation on the control plate. In contrast, cells seeded onto the plates coated by the coiled-coil formation showed a steady proliferation until day 4 after (Fig. 7) which, cell growth decreased rapidly. This result showed that the release of the complex structure protein could diffuse for 4 days. These findings indicated that helixA-scVEGF121 has functionally intact VEGF activity without impairment caused by fusion and the coiled-coil assembly formed with CBDEREI2-helixB. This demonstrated that the formed compound was bifunctional with both collagen-binding property and VEGF activity.

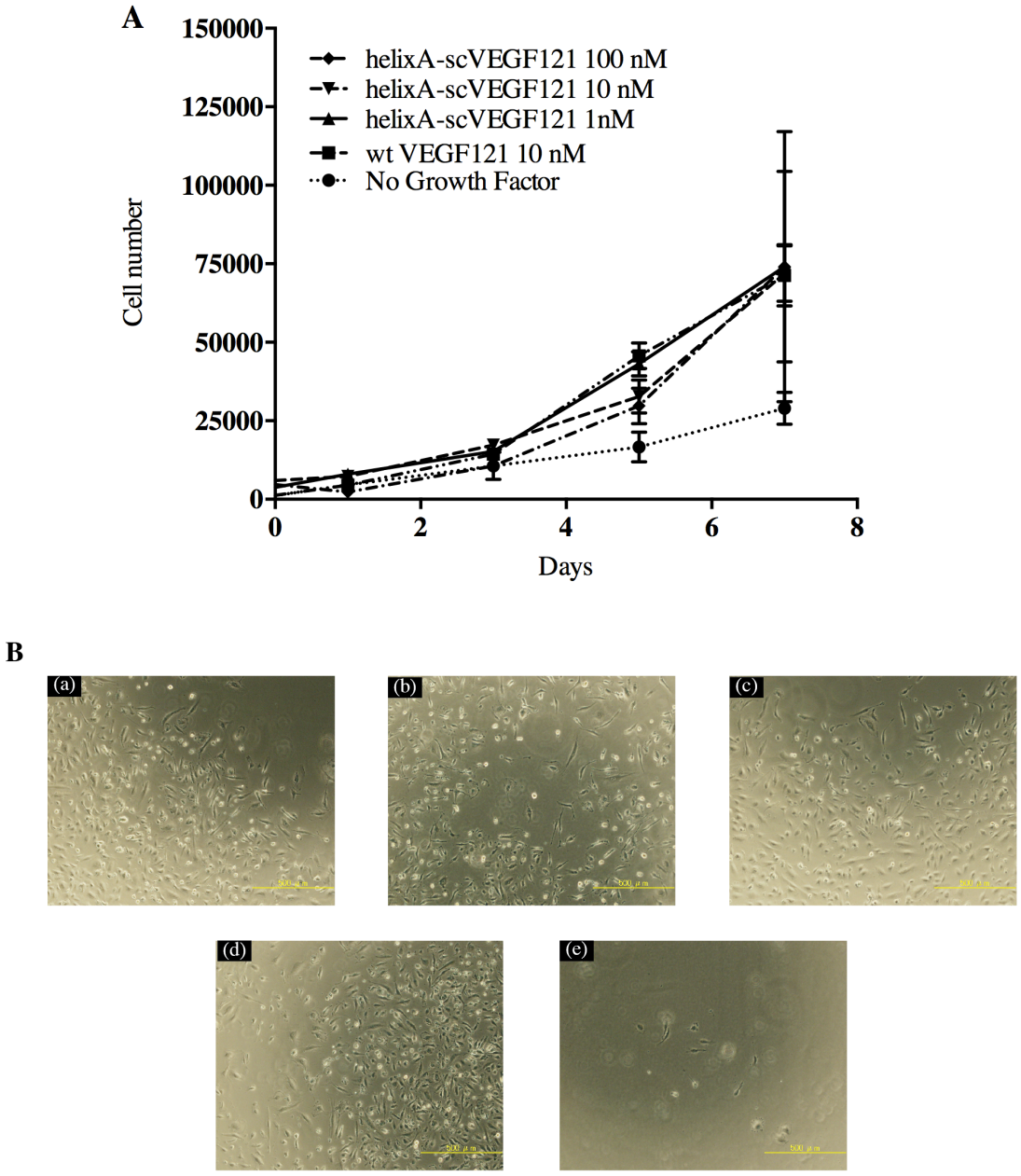

Figure 6: Cell growth activities of free form helixA-scVEGF121. (A) Various concentrations of helixA-scVEGF121 were added to the culture medium of HUVEC cells. The number of cells was counted every two days during 7 days. (B) Effect of helixA-scVEGF121 100 nM (a), 10 nM (b), 1 nM (c), wt-VEGF121 (d) when added to the culture medium of HUVECs. Cells were photographed after 7 days of culture by microscopic observations and compared to the negative control, which were cells cultured in a culture medium without growth factors (e). Scale bar = 500 μm.

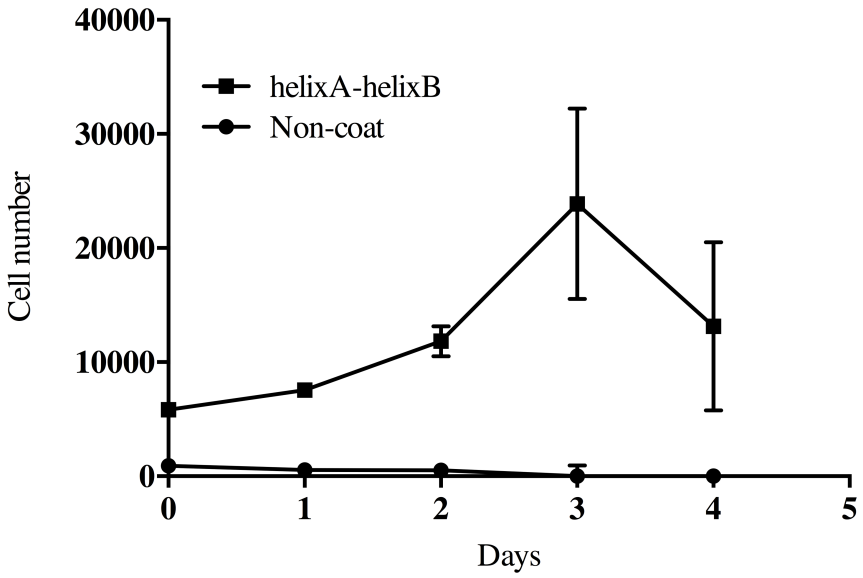

Figure 7: Cell growth on adsorbed helixA-scVEGF$_{121}$. HUVECs were seeded on 24-well non-tissue plate whose surface was treated with helixA-scVEGF$_{121}$ through coated CBDEREI2-helixB. The cell number was evaluated every day during 4 days.

2.3.6. Angiogenic activity of co-immobilized fusion proteins on extracellular matrix

To investigate the activity of our helixA and helixB complex, HUVECs were seeded on five different scaffolds containing different combinations of the coiled-coil structure formation for 4 days (Fig. 8A).

The morphology of HUVECs was monitored (Fig. 8B) and pseudo-tube formation started to form within 2 to 4 hours after they were seeded on ACFEV. This phenomenon was observed on the other scaffolds only after day 1. However, tube-like formations were not observed for the scaffold containing only atelocollagen supplied with HuMedia without growth factors. After 2 days of culture, cells did not survive and detached from the scaffold. To support these observations and confirm angiogenesis activity, markers such as angiopoietin-2 (Ang-2), Tie-2 and matrix metalloproteinase-2 (MMP-2) were analyzed using RT-PCR (Fig. 9). Ang-2 and Tie-2 were selected as an important signaling and transporting ligand/receptor system located in the endothelium of proliferating neovessels [24, 25] and are required to initiate neovascularization. ACF and ACFE showed very low Ang-2 and Tie-2 signals while ACFV and ACFEV expressed the same intensity as the positive control. Moreover, MMP-2 was used as MMPs degrade basal membranes and ECM surrounding the sprouting capillaries to regulate angiogenesis. ACF, ACFE and the positive control showed fairly low expression of MMP-2 while high level of MMP-2 was observed in ACFV and ACFEV. These results indicate that ACFEV exhibited higher rate of migration, invasion of extracellular matrix and capillary-like structure, whereas cells on ACF did not effectively form a network capillary-like structure.

A

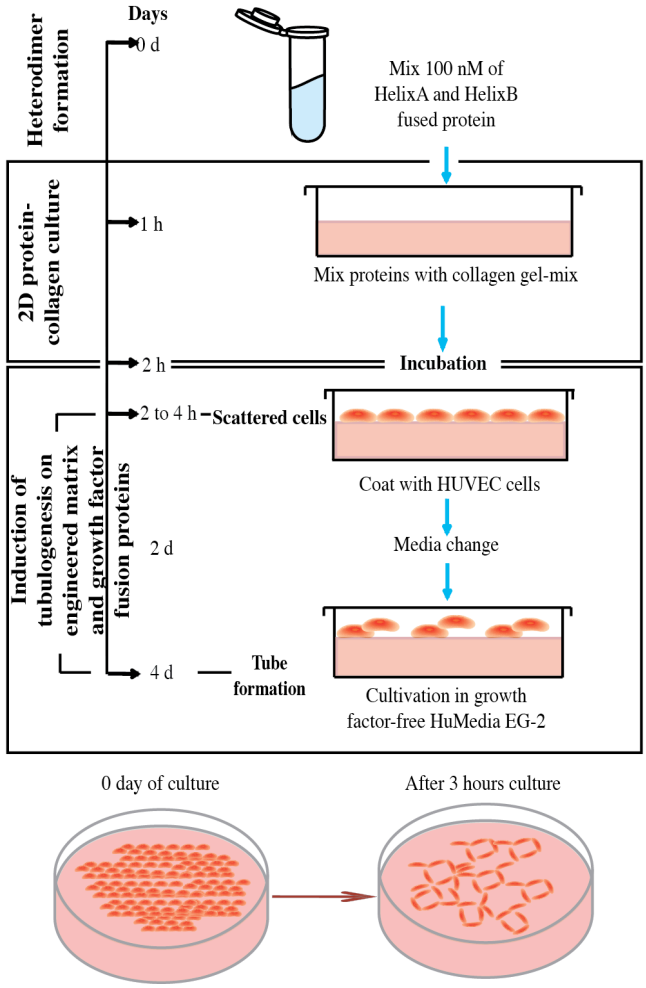

Figure 8: Capillary tube-like formation of HUVECs cultured with constructed ECM and growth factor fusion proteins. (A) Schematic representation of the experimental setup.

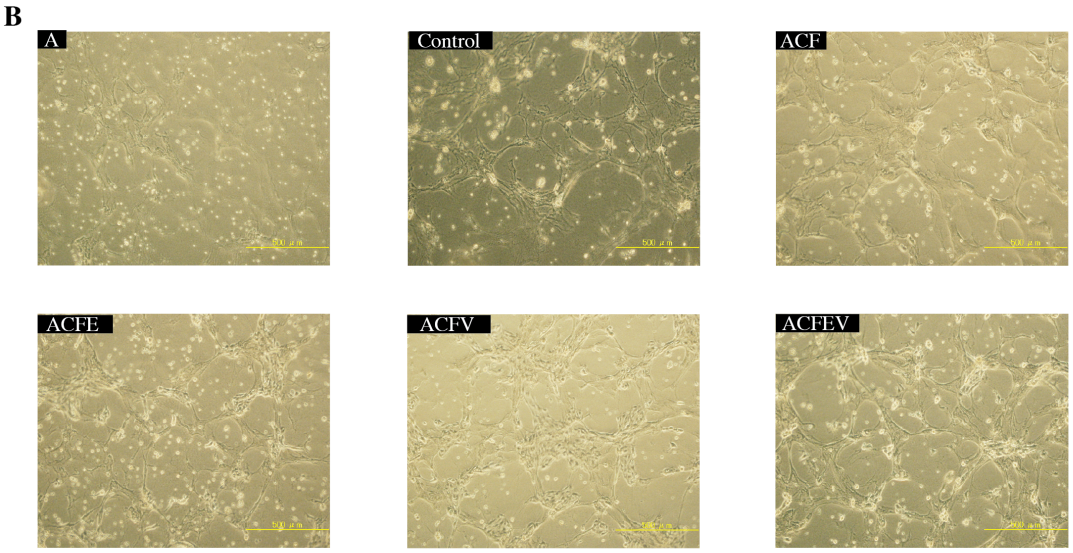

Figure 8: Capillary tube-like formation of HUVECs cultured with constructed ECM and growth factor fusion proteins. (B) Morphology of HUVECs seeded on atelocollagen gel layer. ECM and growth factor fusion proteins through coiled-coil formation embedded in atelocollagen gel was prepared. HUVECs were seeded on the gel-mix. After 2 days of culture, network formation was monitored. A: Atelocollagen, ACF: Atelocollagen+CBDEREI2-helixB+helixA-bFGF, ACFE: Atelocollagen+CBDEREI2-helixB+helixA-bFGF+helix-EGF, ACFV: Atelocollagen+CBDEREI2-helixB+helixA-bFGF+helixA-scVEGF$_{121}$, ACFEV: Atelocollagen+CBDEREI2-helixB+helixA-bFGF+helixA-EGF+helixA-scVEGF$_{121}$. Scale bar = 500 μm.

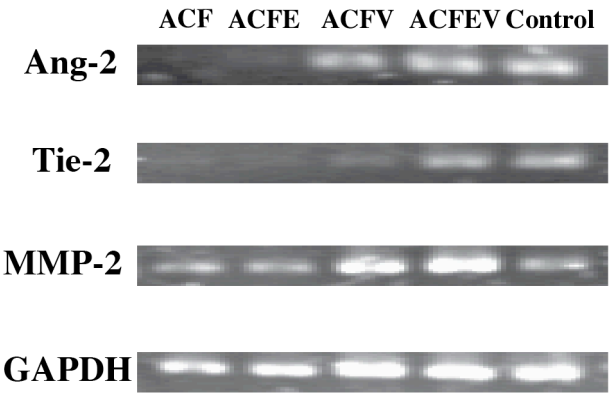

Figure 9: RT-PCR analysis of angiogenic markers. After 4 days of culture on atelocollagen-fusion proteins, HUVECs were harvested and RT-PCR was performed. PCR products were resolved by 1.5% agarose gel electrophoresis. Control means HUVECs in culture medium containing commercial growth factors. Ang-2: angiopoieting-2, MMP-2: matrix metalloproteinase-2.

2.4. Discussion

In this study, our protein engineering approach aimed at co-immobilizing three growth factors via a coiled-coil structure on a collagen scaffold containing our engineered ECM protein to enhance tubular network formation. We demonstrated that the coiled-coil compound formation maintained a steady activity accumulation of both growth factors fusion protein and extracellular matrix fusion protein. This formation also stimulated the growth-promoting activity of HUVECs, improved cell survival, controlled the release of growth factors and promoted capillary-like formation.

The protein binding through coiled-coil structure concluded that the oppositely charged residues contained in helixA and helixB triggered their electrostatic attraction and provided a major driving force for the formation of coiled-coil heterodimers with a leucine zipper [18]. This suggests that the binding of helixA- scVEGF$_{121}$, helixA-bFGF and helixA-EGF to CBDEREI2-helixB was specific. The investigation of the CBDEREI2-helixB conducted on different types of collagen showed that the fusion location of CBD at the C-termini [4] or N-termini (in this case) did not hamper the activity of CBDEREI2-helixB and proved to retain activities on atelocollagen. This observation is in agreement with Sakai and colleagues, which report the use of atelocollagen as a biomaterial. Strong collagen binding affinity was observed with CBDEREI2-helixB compared to that with fnCBD, this was related to the combination of elastin-like polypeptide, RGD sequence and laminin-derived peptide formed by EREI2, which created an artificial connective matrix and increased the binding affinity [26].

To further explain the efficacy of CBDEREI2-helixB, cell adhesion experiments showed that cells adhered better in the presence of CBDEREI2-helixB. This is explained by the strong hydrophobicity of the polyhexapeptide APGVGV sequence, which allowed strong adsorption of CBDEREI2-helixB onto the hydrophobic plate surface. The hydrophilicity of CBDEREI2-helixB enabling cell attachment was accredited to the RGD functional peptide unit that had cell recognition sites as well as the IKVAV sequence, which promoted cell-adhesion, confirming our previously published findings. As such, CBDEREI2-helixB unveiled strong interaction with the endothelial cell surface and can be used as a scaffold.

It is noteworthy that the addition of medium without growth factor is insufficient to promote cell proliferation. This observation led us to conclude that helixA- scVEGF$_{121}$ plays a pivotal role activating integrins mediated by VEGF receptors on the cell surface to trigger cell proliferation. And it confirmed that single-chain VEGF not only possessed mitogenic property but also was functionally equivalent to wild-type VEGF [27]. Additionally, the collagen-culture results demonstrated the successful establishment of a tubular network using ACFEV. As shown by gene expression analysis, Ang-2 signals confirmed the expression of Tie-2 receptor, which facilitated the neovascularization [28]. Cells expressed high level of MMP-2 signals. In other words, MMPs located in the cells and infiltrated areas of neovessels degraded the ECM and cell associated proteins and caused ECM remodeling in the pericellular environment of the cell [29]. Our data suggest the generation of tubulogenesis could be prolonged by using atelocollagen as the diffusion of helixA-scVEGF$_{121}$ was observed for 4 days compared to only 3 days in a control plate.

Here we hypothesized that proteins captured in atelocollagen gel were not easily washed out and showed longer period diffusion compared with simple diffusion-based release. This finding suggested that controlled release of our protein was possible and was in concordance with findings on non-heparin-binding growth factors release [30].

The model we designed allowed us to select growth factors with different targets for improved therapeutic applications. For instance, our study focused on potent synergism between scVEGF$_{121}$, bFGF and EGF in the induction of angiogenesis *in vitro*. It would be interesting to explore other targets in addition to endothelial cells, such as iPS cells or ES cells on cell differentiation. Furthermore, it would be interesting to investigate the co-immobilization of growth factors on nanoparticles through coiled-coil structure-based to form a 3D-scaffold for faster vascularization of the wounded region. Likewise, proteins bound through coiled-coil structure may be used in heterogeneous cell patterning to improve cell signaling and improve cell-sprouting orientation for a controlled vasculogenesis.

2.5. Conclusion

We successfully developed a different way to co-immobilize growth factors on matrix using a non-covalent binding through a coiled-coil structure. The cell proliferation was not inhibited and it promoted angiogenesis. This design of matrix-growth factor delivery system may lead to new advances in tissue engineering and regenerative medicine field.

2.6. References

[1] Carmeliet P. Angiogenesis in health and disease. Nature medicine 2003;9(6):653-60.

[2] Li J, Zhang YP, Kirsner RS. Angiogenesis in wound repair: angiogenic growth factors and the extracellular matrix. Microscopy research and technique 2003;60(1):107-14.

[3] Folkman J, Shing Y. Angiogenesis. The Journal of biological chemistry 1992;267(16):10931-4.

[4] Nakamura M, Mie M, Mihara H, Kobatake E. Construction of multi-functional extracellular matrix proteins that promote tube formation of endothelial cells. Biomaterials 2008;29(20):2977-86.

[5] Kobatake E, Onoda K, Yanagida Y, Aizawa M. Design and gene engineering synthesis of an extremely thermostable protein with biological activity. Biomacromolecules 2000;1(3):382-6.

[6] Karle IL, Urry DW. Crystal structure of cyclic (APGVGV)2, an analog of elastin, and a suggested mechanism for elongation/contraction of the molecule. Biopolymers 2005;77(4):198-204.

[7] Barrera DA, Zylstra E, Lansbury PT, Langer R. Synthesis and Rgd Peptide Modification of a New Biodegradable Copolymer - Poly(Lactic Acid-Co-Lysine). J Am Chem Soc 1993;115(23):11010-1.

[8] Cook AD, Hrkach JS, Gao NN, Johnson IM, Pajvani UB, Cannizzaro SM, et al. Characterization and development of RGD-peptide-modified poly(lactic acid-co-lysine) as an interactive, resorbable biomaterial. Journal of biomedical materials research 1997;35(4):513-23.

[9] Tashiro K, Sephel GC, Weeks B, Sasaki M, Martin GR, Kleinman HK, et al. A Synthetic Peptide Containing the Ikvav Sequence from the a-Chain of Laminin Mediates Cell Attachment, Migration, and Neurite Outgrowth. Journal of Biological Chemistry 1989;264(27):16174-82.

[10] Kibbey MC, Grant DS, Kleinman HK. Role of the SIKVAV site of laminin in promotion of angiogenesis and tumor growth: an in vivo Matrigel model. Journal of the National Cancer Institute 1992;84(21):1633-8.

[11] Schnaper HW, Kleinman HK, Grant DS. Role of laminin in endothelial cell recognition and differentiation. Kidney international 1993;43(1):20-5.

[12] Charriere G, Bejot M, Schnitzler L, Ville G, Hartmann DJ. Reactions to a bovine collagen implant. Clinical and immunologic study in 705 patients. Journal of the American Academy of Dermatology 1989;21(6):1203-8.

[13] Sakai D, Mochida J, Iwashina T, Watanabe T, Suyama K, Ando K, et al. Atelocollagen for culture of human nucleus pulposus cells forming nucleus pulposus-like tissue in vitro: influence on the proliferation and proteoglycan production of HNPSV-1 cells. Biomaterials 2006;27(3):346-53.

[14] Ishikawa T, Terai H, Kitajima T. Production of a biologically active epidermal growth factor fusion protein with high collagen affinity. Journal of biochemistry 2001;129(4):627-33.

[15] Klenkler BJ, Griffith M, Becerril C, West-Mays JA, Sheardown H. EGF-grafted PDMS surfaces in artificial cornea applications. Biomaterials 2005;26(35):7286-96.

[16] Boucher C, Ruiz JC, Thibault M, Buschmann MD, Wertheimer MR, Jolicoeur M, et al. Human corneal epithelial cell response to epidermal growth factor tethered via coiled-coil interactions. Biomaterials 2010;31(27):7021-31.

[17] Kobatake E, Takahashi R, Mie M. Construction of a bFGF-tethered extracellular matrix using a coiled-coil helical interaction. Bioconjugate chemistry 2011;22(10):2038-42.

[18] O'Shea EK, Lumb KJ, Kim PS. Peptide 'Velcro': design of a heterodimeric coiled coil. Current biology : CB 1993;3(10):658-67.

[19] O'Shea EK, Rutkowski R, Stafford WF, 3rd, Kim PS. Preferential heterodimer formation by isolated leucine zippers from fos and jun. Science 1989;245(4918):646-8.

[20] Pepper MS, Ferrara N, Orci L, Montesano R. Potent synergism between vascular endothelial growth factor and basic fibroblast growth factor in the induction of angiogenesis in vitro. Biochemical and biophysical research communications 1992;189(2):824-31.

[21] Nillesen ST, Geutjes PJ, Wismans R, Schalkwijk J, Daamen WF, van Kuppevelt TH. Increased angiogenesis in acellular scaffolds by combined release of FGF2 and

VEGF. Journal of controlled release : official journal of the Controlled Release Society 2006;116(2):88-90.

[22] Noda T, Kawamura R, Funabashi H, Mie M, Kobatake E. Transduction of NeuroD2 protein induced neural cell differentiation. Journal of biotechnology 2006;126(2):230-6.

[23] Elloumi I, Kobayashi R, Funabashi H, Mie M, Kobatake E. Construction of epidermal growth factor fusion protein with cell adhesive activity. Biomaterials 2006;27(18):3451-8.

[24] Holash J, Maisonpierre PC, Compton D, Boland P, Alexander CR, Zagzag D, et al. Vessel cooption, regression, and growth in tumors mediated by angiopoietins and VEGF. Science 1999;284(5422):1994-8.

[25] Zagzag D, Hooper A, Friedlander DR, Chan W, Holash J, Wiegand SJ, et al. In situ expression of angiopoietins in astrocytomas identifies angiopoietin-2 as an early marker of tumor angiogenesis. Experimental neurology 1999;159(2):391-400.

[26] Bonzon N, Carrat X, Deminiere C, Daculsi G, Lefebvre F, Rabaud M. New artificial connective matrix made of fibrin monomers, elastin peptides and type I + III collagens: structural study, biocompatibility and use as tympanic membranes in rabbit. Biomaterials 1995;16(11):881-5.

[27] Boesen TP, Soni B, Schwartz TW, Halkier T. Single-chain vascular endothelial growth factor variant with antagonist activity. The Journal of biological chemistry 2002;277(43):40335-41.

[28] Asahara T, Chen D, Takahashi T, Fujikawa K, Kearney M, Magner M, et al. Tie2 receptor ligands, angiopoietin-1 and angiopoietin-2, modulate VEGF-induced postnatal neovascularization. Circulation research 1998;83(3):233-40.

[29] Kvanta A, Sarman S, Fagerholm P, Seregard S, Steen B. Expression of matrix metalloproteinase-2 (MMP-2) and vascular endothelial growth factor (VEGF) in inflammation-associated corneal neovascularization. Experimental eye research 2000;70(4):419-28.

[30] Sakiyama-Elbert SE, Hubbell JA. Controlled release of nerve growth factor from a heparin-containing fibrin-based cell ingrowth matrix. Journal of controlled release : official journal of the Controlled Release Society 2000;69(1):149-58.

Chapter 3

Nanoparticle-Growth factor interaction through coiled-coil formation: A promising biomaterial for targeted drug delivery

---

"A scientist in his laboratory is not a mere technician: he is also a child confronting natural phenomena that impress him as though they were fairy tales." – Marie Curie

3.1 Introduction

Recently researchers have turned their focus to protein-mediated drug delivery by developing various biodegradable and non-biodegradable systems such as adenoviruses, microparticles, microspheres, hydrogels and nanoparticles [1-3]. However, challenges to overcome protein stability, antigenicity and drug absorption through epithelial barrier are still under investigation [4, 5]. Protein biomaterials like silk, lysozyme, PEGylated and elastin-like polypeptides (ELP) assembled into particles have been developed to a great extend for therapeutic applications [6-8].

In order to properly deliver small molecules within cells, nano-scale particles have been frequently used as drug carriers. Nanoparticles have been designed in such a way that the core was hydrophobic and were covalently coupled to their polymer-carrier without the activity being hampered [9-11]. Nevertheless, limitations using covalent binding techniques might be encountered for instance biological activity loss or adsorption limitations of cell adhesion [12, 13]. Moreover, in case of cancer treatment, high radiation doses are required to break down covalent bonds [14]. Delivering drugs using a covalently conjugated carrier might result in unspecific uptake of healthy cells resulting in damaging healthy tissues. Only few studies have been carried out by non-covalent conjugation strategies [15].

Accordingly, in this investigation, a drug delivery system consisting of applying any type of growth factor conjugated non-covalently to an elastin-like nanoparticle has been developed. This nanoscale protein has a thermo-responsive, biocompatible and biodegradable elastin-like polypeptide $(PAVGV)_{42}$ conjugated to a polyaspartic acid D_{44}. The addition of polyaspartic acid [16] seems to confer the ELP with a stabilized assembly at the phase transition temperature, rendering the particle surface negative-charged and therefore preventing intrinsic particle aggregation. The reason of choosing poly(PAVGV) over poly(PGVGV) is due to the non-reversibility of poly(PAVGV) following the particle formation [16, 17]. Moreover, it has been reported that this striking repetition of (PAVGV) has an extremely high biocompatibility features. Due to these characteristics, the polymer cannot be differentiated by the immune system from the natural elastin [17]. Therefore, utilizing ELPs as drug delivery vehicle allows a safe platform to a controlled drug release.

The non-covalent model relies on two peptides; ACID-p1 (helixA), which has been fused to growth factors and, BASE-p1 (helixB) fused with the nanoparticle (Fig. 1). HelixA and helixB were developed by O'Shea and colleagues according to the Fos/Jun leucine zipper, which forms a favorable heterodimer formation under unfavorable interhelical electrostatic destabilization of the homodimer structure [18, 19].

This coiled-coil formation probably demonstrates the utmost diversity of protein-protein interactions in terms of geometry, orientation and sequence arrangement favoring effortless pairing of two right-handed α-helices.

In this study, we developed a unique strategy to deliver drugs non-covalently by choosing growth factors according to receptor types present on cell surface, in other words, the flexibility of changing a protein moiety according to targeted area without altering the drug vehicle with respect to biocompatibility.

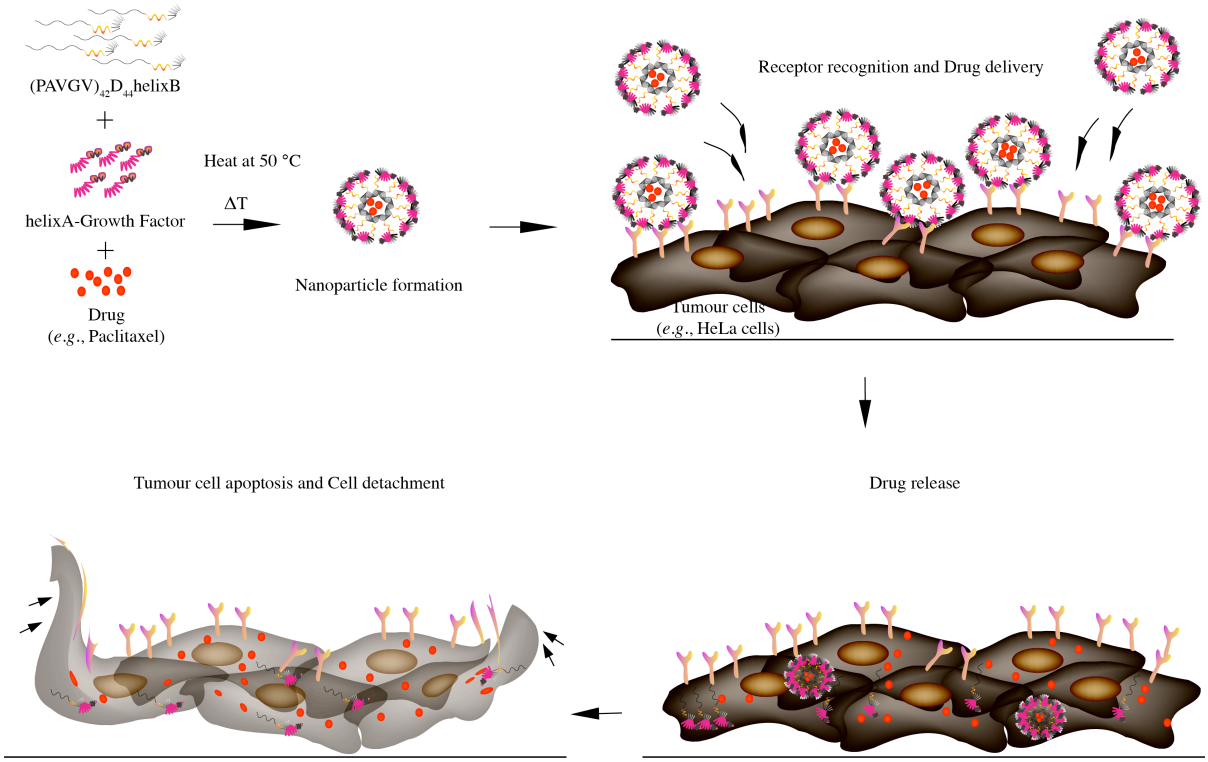

Figure 1: Schematic illustration of non-covalent binding of the designed thermo-responsive ELP nanoparticle to growth factor through coiled-coil structure for drug delivery and release

3.2 Materials and methods

3.2.1 Plasmid Construction

The DNA sequence of $(PAVGV)_7$ was obtained by elongating hybridized DNA oligonucleotides,5'-CAGGGATCCCGGCCGTTGGTGTACCGGCCGTTGGTGTGCCG

GCCGTTGGTGTTCCGGCGGTAGGCGTACCGGCGGTAGGCGTGCCGGCGG-3' and 5'-GCCGTCGACCAAGATCTTAACACCTACGGCCGGAACGCCCACGGCCGGCAC

GCCCACCGCCGGTACGCCCACCGCCGGAACGCCTACCGCCGGCACGCCTACCG CC -3', and cloned into pBluescript II SK(+) (Stratagene) using *Bam*HI and *Sca*I restriction enzymes. Same procedure has been repeated to obtain $(PAVGV)_{42}$. Lysine and isoleucine amino acids were introduced between each 7 repeats of (PAVGV) portion.

Polyaspartic acid fragment was obtained from pET28b-$(GVGVP)_{36}$-Dm-CHis (m=22, 44, 88, 176) constructed previously [20]. $(PAVGV)_{42}$ fragment was then inserted after removal of $(GVGVP)_{36}$ fragment using *Bam*HI and *Sal*I to obtain pET28b-$(PAVGV)_{42}$-D_{44}-CHis plasmids.

To get pET28b-$(PAVGV)_{42}$-D_{44}-helixB-CHis, helixB fragment from pET-GGGS4-helixB previously constructed was amplified by PCR using a pair of primers containing *Xho*I restriction enzymes and was inserted in pBS phagemid. pBS-GGGS4-helixB and pET28b-$(PAVGV)_{42}$-D_{44}-CHis were digested using *Xho*I enzyme. HelixB fragment was then inserted in pET28b-$(PAVGV)_{42}$-D_{44}-CHis (PD). pET28b-$(PAVGV)_{42}$-D_{44}-helixB (PDB) was confirmed by sequencing. All primers used in this experiment see Table 1.

Table 1: HelixB primers used for plasmid construction.

Primer	Forward primer (5' – 3')	Reverse primer (5' – 3')
helixB	AAGCTTctcgagTGGATCcgcggtgga	AAGCTTctcgagTGGATCTAACTTTTTC

3.2.2 Expression and purification of fusion proteins

pET28b-$(PAVGV)_{42}$-D_{44}-CHis and pET28b-$(PAVGV)_{42}$-D_{44}-helixB-CHis plasmids were transfected into *E.coli* KRX competent cells by heat shock and cultured at 37 °C in a

Luria-Bertani (LB) medium supplemented with ampicillin to an optical density of 0.6 at 600 nm. Protein expression was induced by addition of 1 mM isopropylthio-ß-D-galactoside (IPTG) and 0.1% rhamnose. Cells were cultured overnight at 30 °C, harvested by centrifugation (9 000 g) and resuspended in Bug Buster Reagent and Benzonase nuclease followed by rotation at room temperature for 30 min before repelleting by centrifugation (9 000 g) for 10 min.

Protein extraction from soluble fraction: The supernatant was collected and purified by His select TALON Metal Affinity Resins (Clontech) using a Poly prep column (Bio-Rad). After 30 min incubation at 4 °C, the column was washed three times with four-column volumes of the wash buffer (50 mM sodium phosphate, 300 mM NaCl, pH 7.6) and followed by three times with four volumes of the same buffer including 5 and 10 mM imidazole each. The fusion proteins were eluted with two-column volume of elution buffer (50 mM sodium phosphate, 300 mM NaCl, 100 mM imidazole, pH 7.6). The fusion proteins were then dialyzed in a PBS buffer overnight using a Slider-A-lyzer dialysis cassette 10,000 MWCO (PIERCE).

Protein extraction from inclusion bodies: The supernatant was discarded and the proteins were extracted from the inclusion bodies and solubilised with 8 M Urea PBS for overnight at 4 °C. The supernatant was collected by centrifugation (9 000 g) for 10 min and purified by His select TALON Metal Affinity Resins (Clontech) using a Poly prep column (Bio-Rad). After 30 min incubation at 4 °C, the column was washed three times with four-column volumes of the wash buffer (50 mM sodium phosphate, 300 mM NaCl, 4 M Urea, pH 7.6) and followed by three times with four volumes of the same buffer including 5 mM imidazole. The fusion proteins were eluted with two-column volume of elution buffer (50 mM sodium phosphate, 300 mM NaCl, 4 M Urea, 100 mM imidazole, pH 7.6).

3.2.3 Evaluation of protein binding through coiled-coil structure

To show the specific binding between helixA and helixB as well as the optimum concentration of our fusion proteins to be used in further experiments, 96-well ELISA plates (Costar 3361, Corning Life sciences, Lowel, MA), were coated for overnight at 4 °C

with 100 nM of PDB. Plates were washed 3 times with PBS-T and blocked overnight with 2% bovine serum albumin (BSA) in PBS buffer at 4 °C. After blocking, plates were washed again and incubated with increased concentrations of helixA-scVEGF$_{121}$ (10, 50, 100, 500, 1000 nM) for 1 h at 37 °C. After washing, anti-VEGF$_{121}$ (Abcam Life Sciences, Cambridge, MA), was reacted for 1 h at 37 °C. HRP-conjugated secondary IgG at 1:1000 dilution was added and reacted for 1 h at 37 °C. TMB peroxidase substrate (KPL, Gaithersburg, MD) was added after washing three times with PBS-T and reaction was stopped after 5 min by adding 1 N HCl. The binding was detected and measured spectrophotometrically at a wavelength of 450 nm (Benchmark, Bio-Rad).

3.2.4 Turbidimetry

The optical density of the aqueous polymer solutions was monitored in the region 190-800 nm using a temperature-controlled UV/VIS spectrophotometer (Beckman DU7500). The starting temperature was set at 20 ºC to slowly increase by 1 ºC/min to a final temperature of 50 ºC. Reverse measurement was also monitored. The concentration of the proteins applied was 200 μg/ml. The solutions were equilibrated for about 5 min prior to measurement. Proteins and reagents were filtered using a 0.22 μm filter (Millipore). All spectroscopic measurements were performed in quartz glass cuvettes.

3.2.5 Dynamic light scattering (DLS)

The size of the PD and PDB nanoparticles formed in dilute acqueous solutions at 20 ºC and 50 ºC were determined by means of a NanoZetasizer, Nano-ZS Malvern apparatus. PBS was filtered through 0.22 μm filter to remove any large impurity particulates. The proteins were diluted with the filtered PBS to a final concentration of 500 μg/ml. Proteins were flowed into the flow cell to determine the nanoparticle size. Light scattering measurements were taken for at least 3 to 10 runs. The excitation light source was a 4 mW He-Ne laser at 633 nm, and the intensity of the scattered light was measured at 90 ºC. The sizes of the proteins were calculated based on the assumption that the viscosity of PBS was the same as that of water. The size with single-peaked distribution of the nanoparticles was determined by the cumulant algorithm software.

3.2.6 Transmission electron microscopy (TEM)

TEM samples were diluted and dissolved in filtered PBS to a final concentration of 300 μg/ml. Particle fixation involved incubation of the diluted samples at 25 ºC or 50 ºC for 10 min, followed by addition of glutaraldehyde solution to a final concentration of 1% and incubation at the same temperatures for 30 min. The solutions containing the particles were then dialyzed overnight to dialyzed water at 4 ºC to remove unreacted glutaraldehyde. The fixed particles were placed on a carbon-coated copper grid for 10 min at room temperature and stained by negative staining method using phosphotungstate or uranyl acetate for 30 s. Stained samples were dried on filter paper at room temperature for 2 h or more. Grids were examined in a H-7500 (Hitachi) TEM at 80 kV. The digital images were acquired with a charge coupled device camera.

3.2.7 Adsorption of 1,8-ANS

To quantify the adsorption of the fluorescence probe magnesium 1-anilinonaphthalene-8-sulfonate (1,8-ANS) (Nacalai Tesque, Japan) into the nanoparticles, proteins and 1,8-ANS were mixed in PBS. The concentrations of the proteins and 1,8-ANS were 300 μg/ml and 100 μM respectively. The samples were measured in optically clear polystyrene microcuvettes (Bio-Rad, CA) on a fluorescence spectrofluorometer (FP-6500 Jasco, Japan) with an excitation wavelength of 370 nm and an emission wavelength scanning from 400 to 650 nm where the emission at 480 nm was collected.

3.2.8 Fusion protein activity and cell apoptosis

HeLa cells resuspended in Dulbecco's modified eagle medium, DMEM (Gibco's, USA) containing 10% FBS and 1% PS were seeded in 35 mm diameter glass bottomed culture dish (Iwaki, Japan) at a density of 5 x 10^4 cells/dish. After cell attachment to the culture dish, purified PD, PDB, PDB+HA-scVEGF$_{121}$ and PDB+HA-EGF incorporated with paclitaxel (PTX) were added to cell media in 1:1 ratio. HeLa cells without proteins and cells with paclitaxel were considered as negative control and positive control respectively. The concentrations were 1 μM for PD, PDB, HA-scVEGF$_{121}$ and HA-EGF

and 10 μM for PTX. The day on which proteins were added was considered as day 0. To evaluate protein efficacy on cells, calcein-AM and propidium iodide were used to stain viable and dead cells respectively on day 2 and day 4. Fluorescent images were acquired using fluorescence microscopy (IX-70 Olympus, Japan).

3.3 Results

3.3.1 Expression of fusion proteins

The purpose being to develop a nanoparticle having binding abilities to several proteins (eg: growth factors, extracellular matrices, etc.) non-covalently, a fusion protein containing the repetitive sequence (PAVGV), the polyaspartic acid sequence and helix B was engineered to obtain $(PAVGV)_{42}$-D_{44}-helixB. A His-tag was fused to $(PAVGV)_{42}$-D_{44} at the C-terminus under control of T7 promoter. Furthermore helixB was introduced at the C-terminus of the fused protein. The expression of PDB was induced by 1 mM IPTG at 30 °C for 4 hours, and the expressed protein was purified from the soluble and the insoluble fraction of the cell lysate by TALON metal affinity resin. The purity of the fusion proteins was analyzed with 12% SDS-PAGE. The result validated the expected size ranges: $(PAVGV)_{42}$-D_{44} (26.7 kDa) and $(PAVGV)_{42}$-D_{44}-helixB (31.5 kDa). The experimental results are consistent with the calculated molecular masses. The fusion proteins were purified enough for further experiment, as indicated by SDS-PAGE (Fig. 2).

3.3.2 Influence of temperature variation on PD and PDB nanoparticles

The turbidity measurement was performed at pH ~7.4. Temperature variation from 20 °C up to 50 °C and then down to 20 °C was applied to evaluate the thermo-responsivity and the stability of the structure regarding the folding/unfolding ability of the nanoparticles. The results of temperature turbidity are plotted in Figure 3. Phase transition temperature measurements of PD and PDB showed a sudden increase of the absorbance value. Low critical solution temperature (LCST) was determined as the initial break point at which, nanoparticles formation was formed at 37.6 °C and 32.7 °C respectively. Over the mentioned LCSTs, a constant curve is maintained up to 50 °C. Reverse readings showed that cooling down to 20 °C did not prompt the structure of nanoparticles to unfold and therefore preserved a steady absorbance reading.

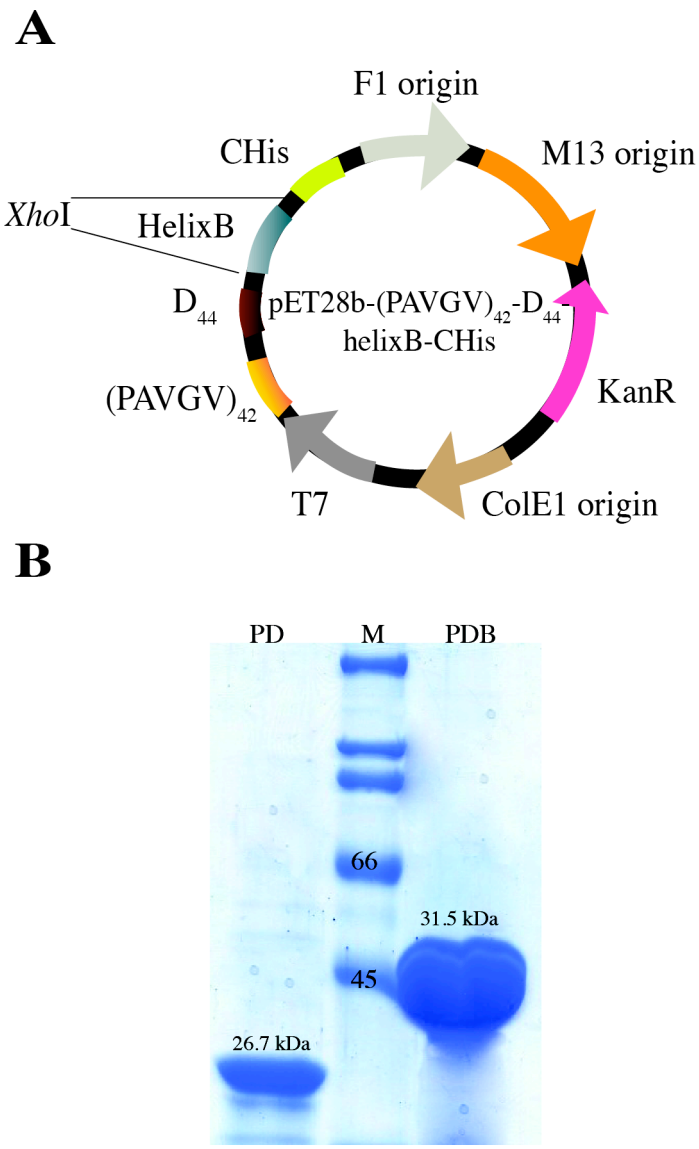

Figure 2: Purification of $(PAVGV)_{42}D_{44}$ and $(PAVGV)_{42}D_{44}$helixB. (A) Constructed plasmids pET28-$(PAVGV)_{42}D_{44}$-CHis and pET28-$(PAVGV)_{42}D_{44}$ helixB-CHis. Fused fragments were cloned into pET-28 backbone under the regulation of T7 promoter. Histidine tag sequence (His-tag) at C-terminus was used for purification of the recombinant protein. (B) SDS-PAGE of purified proteins. Legend: M: marker; PD: $(PAVGV)_{42}D_{44}$ and PDB: $(PAVGV)_{42}D_{44}$helixB.

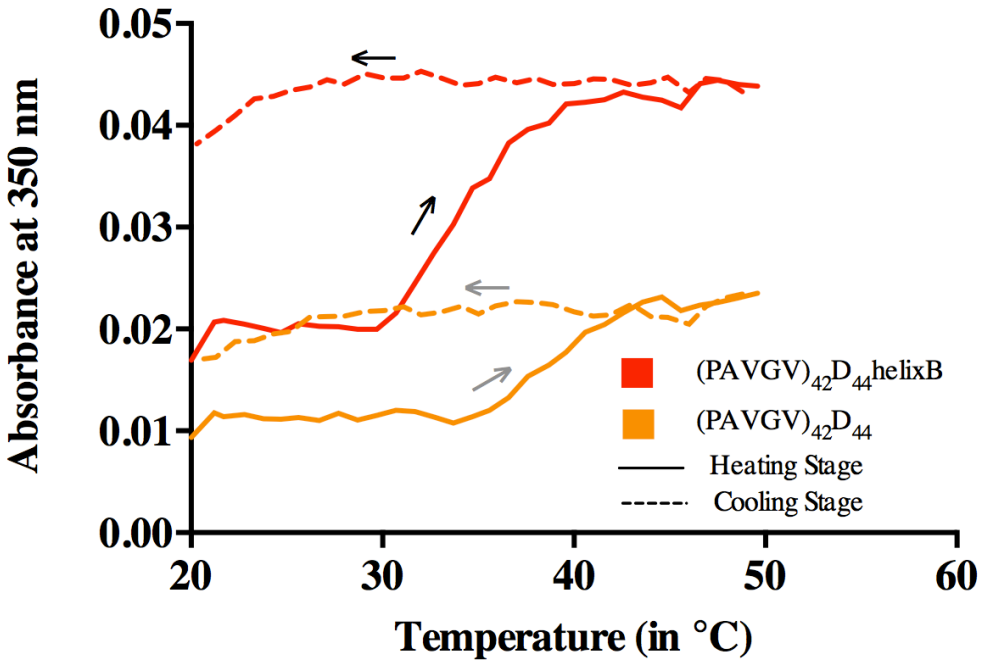

Figure 3: Turbidity (OD_{350}) of $(PAVGV)_{42}D_{44}$ (PD) and $(PAVGV)_{42}D_{44}$helixB (PDB). The turbidity profiles of the polypeptides were obtained at a rate of 1 ºC/min. Heating and cooling profiles were marked by arrows.

3.3.3 Morphological study of PD and PDB nanoparticles

The average hydrodynamic diameter of the nanoparticles was determined by dynamic light scattering measurements (Fig. 4). Nanoparticles underwent measurements at 25 °C, 50 °C and again 25 °C. At 25 °C, PD and PDB particles showed a peak that corresponds to 10 and 13 nm in diameter respectively. At 50 °C, a peak was observed at 16 and 17 nm respectively. After cooling PD and PDB particles down to 25 °C, peaks at 8 and 17 nm was monitored. The size distribution measurements showed that unlike PD, PDB nanoparticles did not unfold under cooling treatment.

Figure 5 displays the TEM images of the PD and PDB nanoparticles recognized in phosphotungstate (PTA) negative stain at two different temperatures, 25 °C and 50 °C as rounded shaped dots. The particle core size of PDB is seen to be approximately 17.5 ± 2 nm in diameter as estimated from the statistical analyses of the previous section. TEM images demonstrate the presence of multiple nanoparticle formation at 50 °C while only few particles are monitored at 25 °C. A clear difference is shown in particles number in PDB images at 50 °C compared with PD ones.

3.3.4 The potential of 1,8-ANS encapsulation

The potential for encapsulation of drugs within the hydrophobic core of the PD and PDB nanoparticles was investigated using fluorescent probes (Fig. 6). The emission spectra indicated insignificant encapsulation of the probe within the polymer at room temperature. Fluorescence spectroscopy demonstrated that elastin-like polypeptide bind with the fluorescent probe 1-anilinonaphthalene-8-sulfonic acid (1,8-ANS) after the particles were heated at 50 °C. Cooling treatment down to 25 °C was applied to the heated particles and no change in absorbance was recorded.

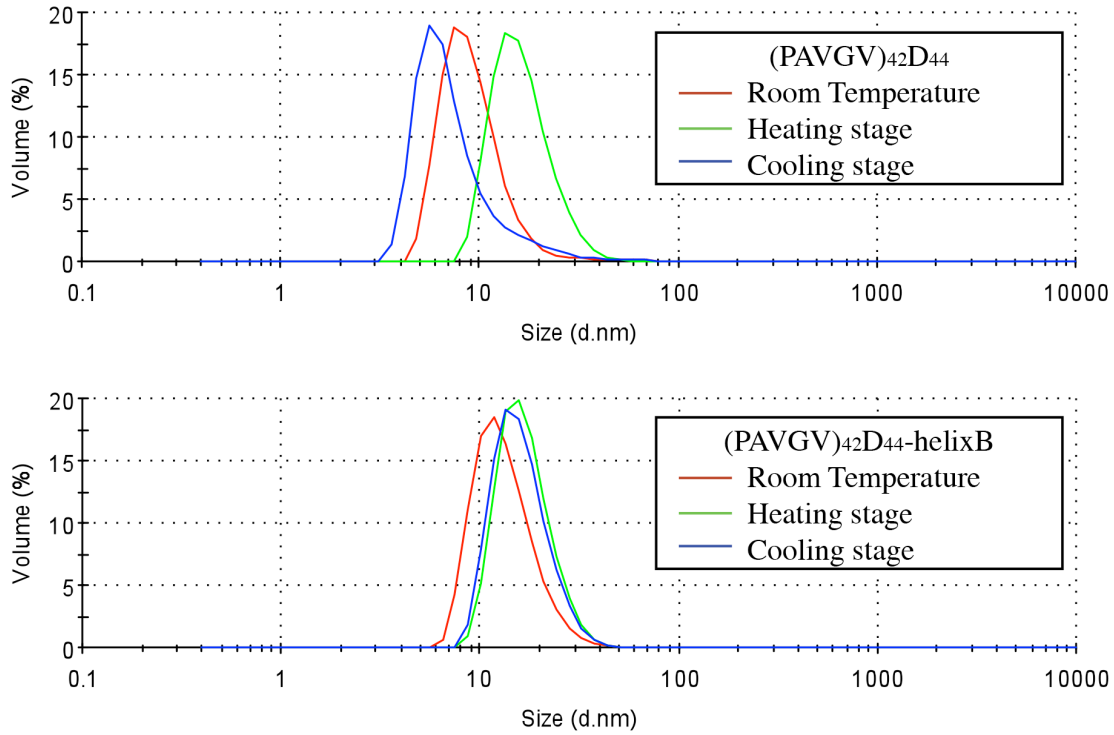

Figure 4: Hydrodynamic size distributions of $(PAVGV)_{42}D_{44}$ and $(PAVGV)_{42}D_{44}$helixB nanoparticles determined using dynamic light scattering. The number average distribution (peak) indicates the average diameter of the nanoparticles.

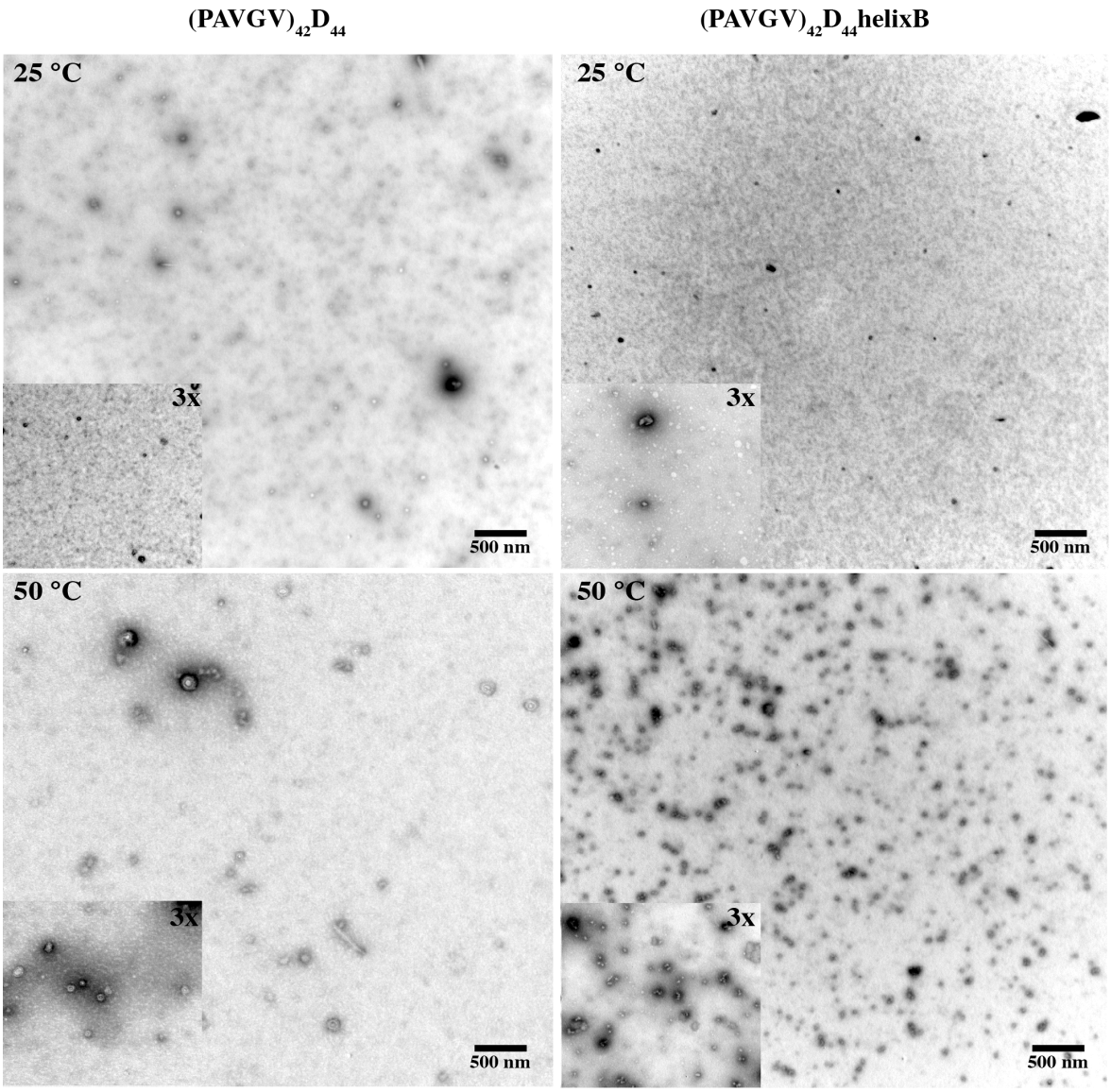

Figure 5: Transmission electron microscopy (TEM) images of $(PAVGV)_{42}D_{44}$ and $(PAVGV)_{42}D_{44}$helixB nanoparticles at 25 ºC and 50 ºC. The particles are polydisperse.

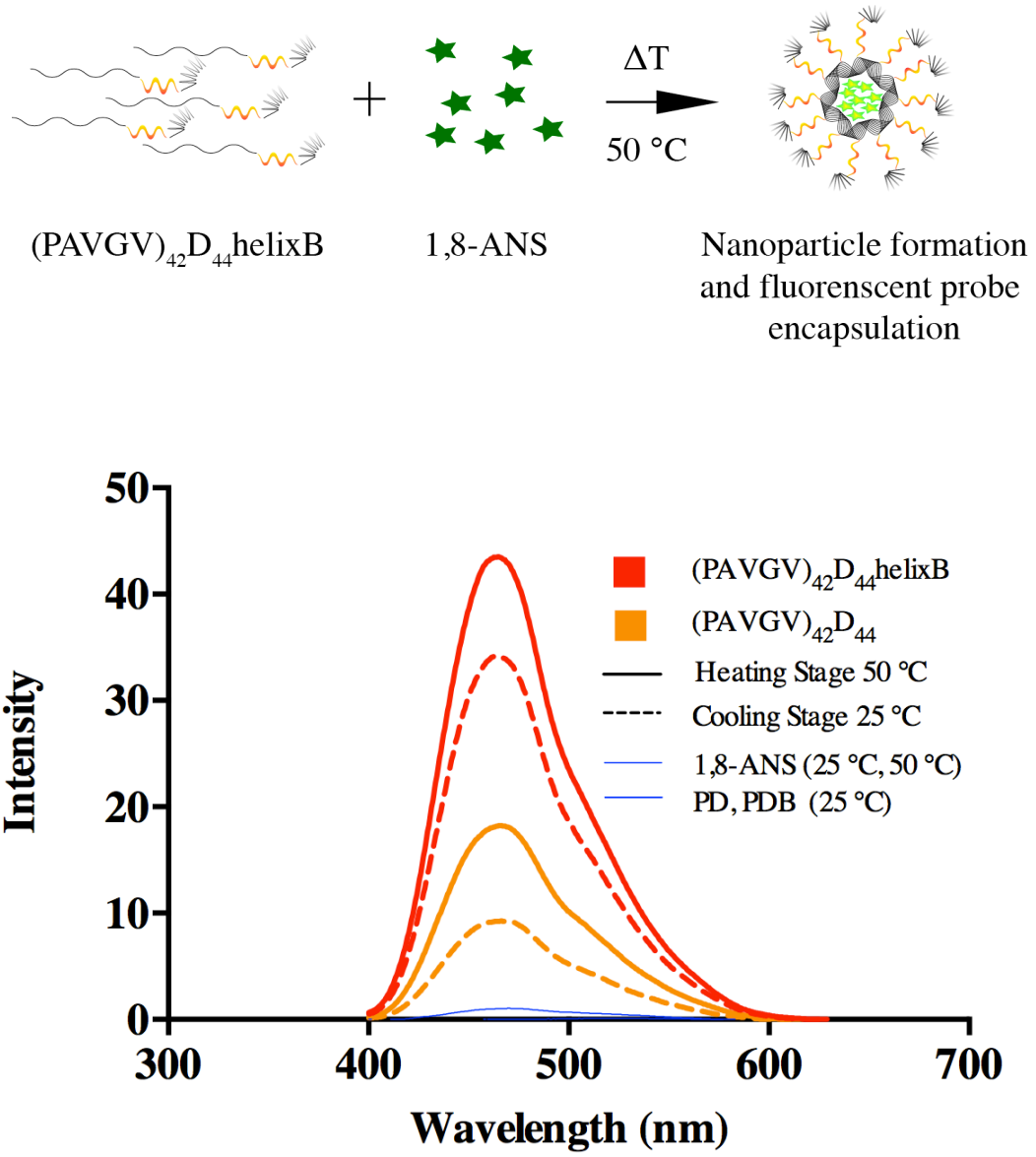

Figure 6: Fluorescence binding profile of $(PAVGV)_{42}D_{44}$ and $(PAVGV)_{42}D_{44}$helixB nanoparticles at 25 ºC and 50 ºC. (A) Schematic illustration of fluorescent probe encapsulation in a hydrophobic environment after heating. (B) Fluorescence emission spectra of 1,8-ANS: dotted curve, 1,8-ANS alone, PD and PDB at 25 ºC (before heating); continuous curve, PD and PDB loaded with 1,8-ANS at 50 ºC; broken curve, PD and PDB in with 1,8-ANS at 25 ºC (cooling stage).

3.3.5 Protein binding through coiled-coil structure

ELISA analysis was performed to examine the binding ability of helixA to helixB. Anti-VEGF antibody was used for detection of helixA-scVEGF$_{121}$ and the signals were enhanced with HRP-conjugated secondary antibody (Fig. 7). The results showed that signal increased in a dose dependent manner up to 1000 nM and demonstrated that 10 nM of fusion protein is enough to trigger the complex formation of helixA and helixB. Furthermore, these results established that the non-covalent binding formed through coiled-coiled structure could function as an effective bridge connecting growth factor fusion protein and particle protein.

1.1.2 In-vitro evaluation of paclitaxel-loaded nanoparticles using coiled-coil complex

To examine if the encapsulation of PTX-loaded nanoparticles induces apoptosis by PTX, cells were stained with calcein-AM and propidium iodide (PI). Untreated HeLa cells showed no evidence of cell death at day 2 and 4 after staining with calcein-AM and PI (Fig. 8). At day 2, fluorescence images show that cell death has occurred with cells treated with PD, PDB, PDB+ helixA-scVEGF$_{121}$ (PDBV) and PDB+EGF (PDBE). Similar observation is demonstrated at day 4 (Fig. 9) where cell density has decreased and cell death has been shown. Unlike negative and positive control, cells treated with PD, PDB, PDBV and PDBE were detached from day 2 and the process continued until day 4 where roughly only few cells remained attached to the culture dish and this phenomena has been outstandingly observed for cells treated with PDBV and PDBE.

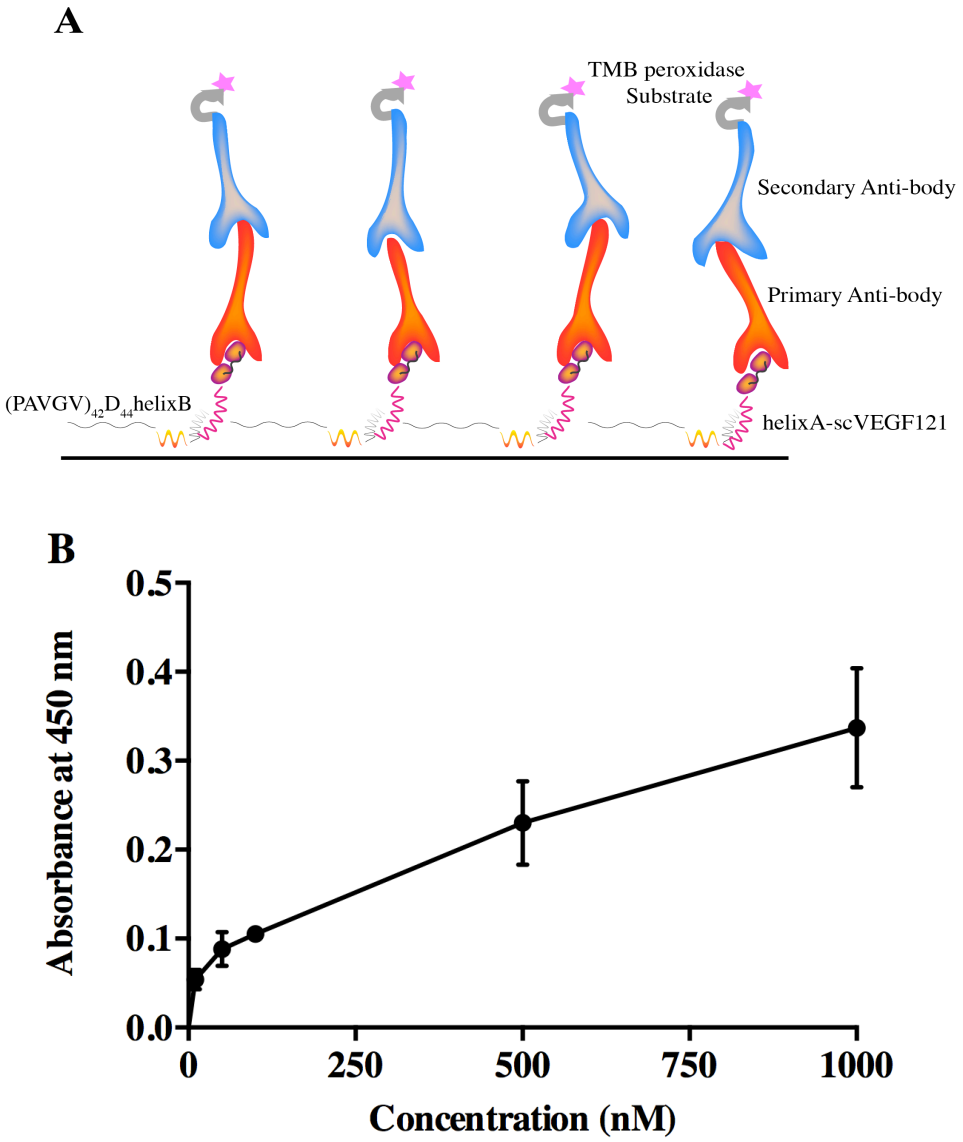

Figure 7: Binding of helixA-scVEGF$_{121}$ to $(PAVGV)_{42}D_{44}$helixB through coiled-coil structure on ELISA plate. (A) Experimental scheme used for ELISA. (B) Various concentrations of helixA-scVEGF$_{121}$ were reacted with $(PAVGV)_{42}D_{44}$helixB adsorbed onto 96-well plate surface. The amounts of bound helixA-scVEGF$_{121}$ were evaluated after HRP IgG binding.

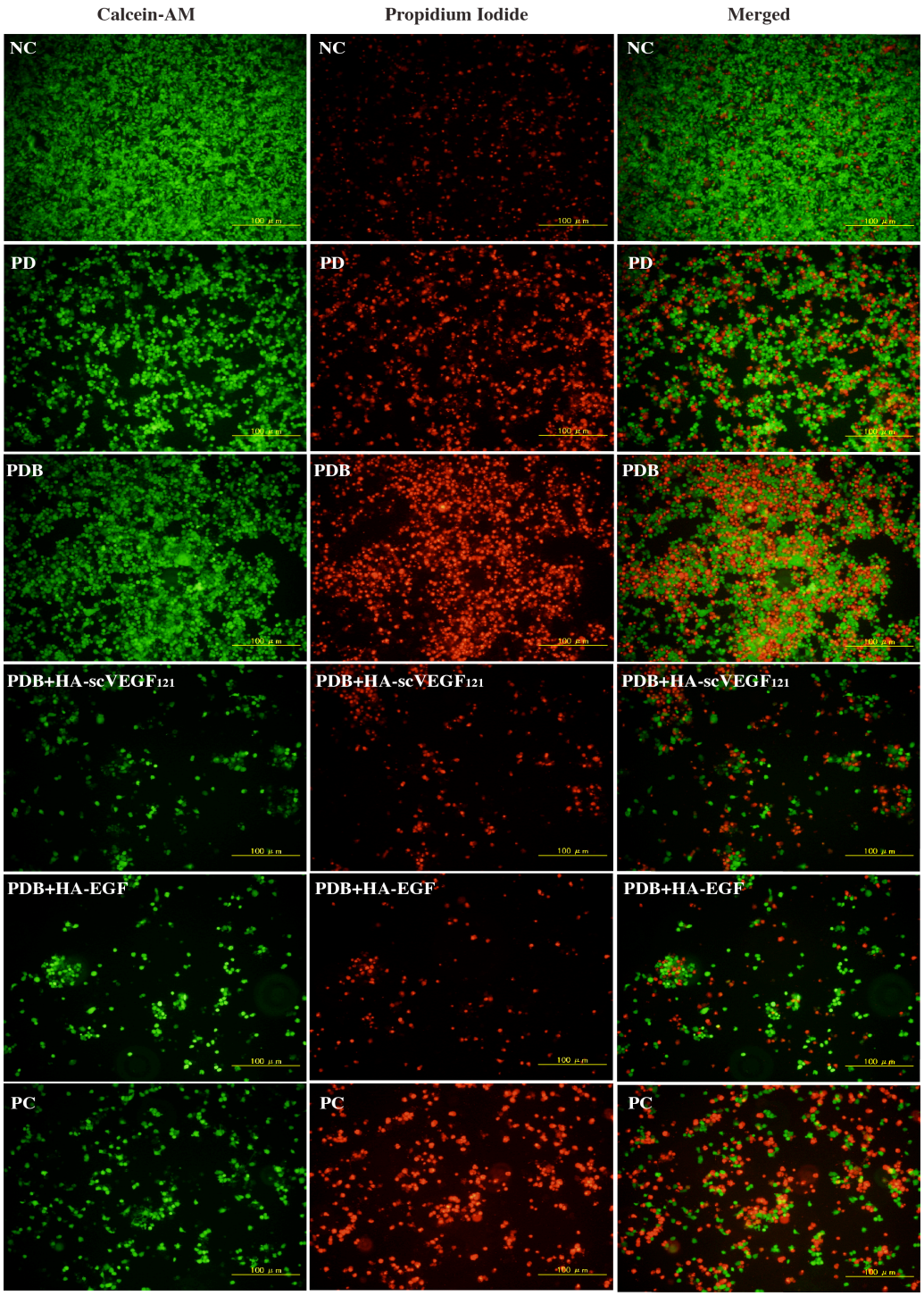

Figure 8: Effect of paclitaxel on HeLa cells 2 days after drug delivery. Fluorescent images showing calcein-AM and propidium iodide staining of cultured HeLa cells treated with nanoparticles (PD, PDB, PDB+HA-scVEGF121 and PDB+HA-EGF) loaded with paclitaxel or direct application of paclitaxel as positive control. Negative control being HeLa cells without addition of paclitaxel.

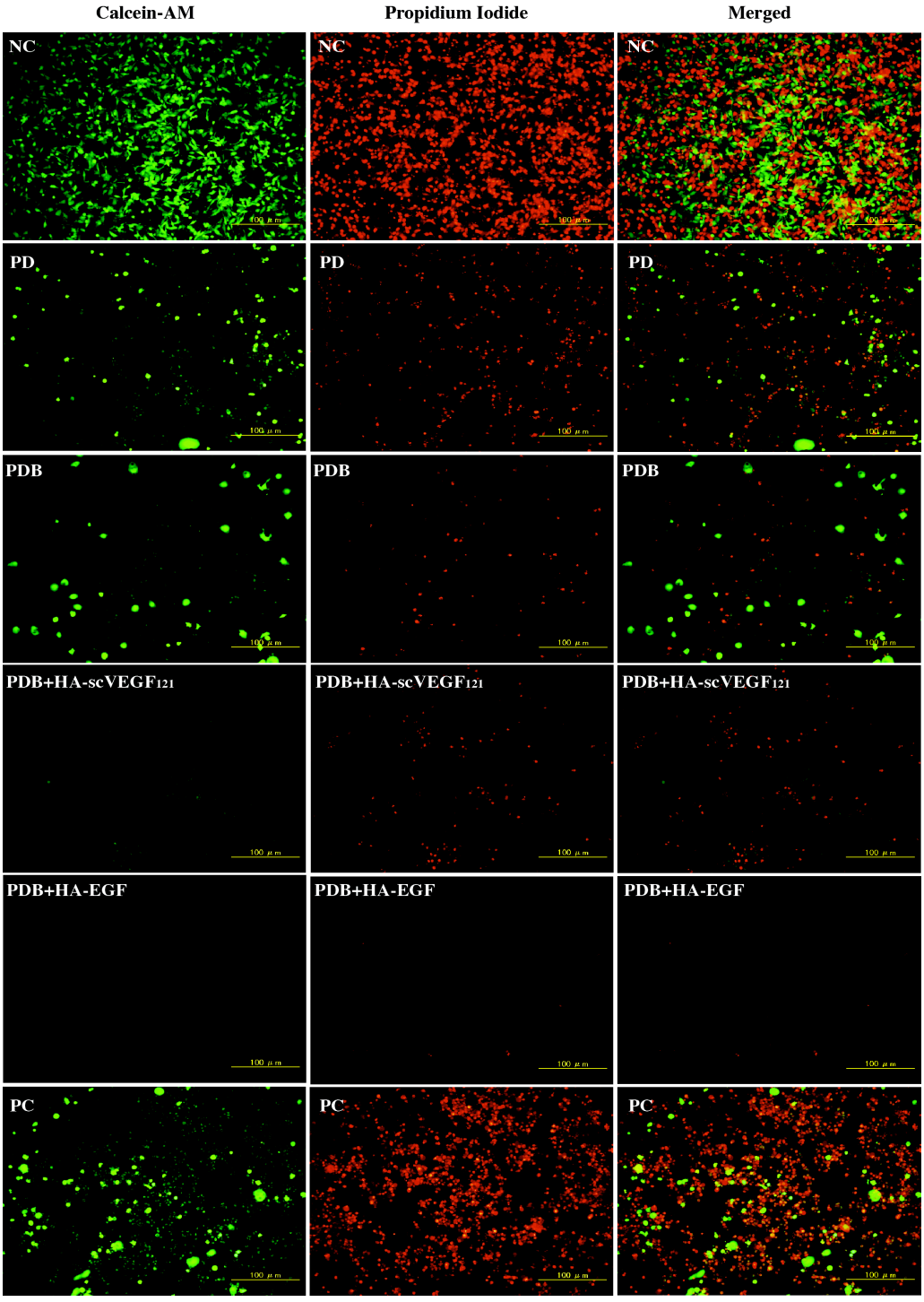

Figure 9: Effect of paclitaxel on HeLa cells 4 days after drug delivery. Fluorescent images showing calcein-AM and propidium iodide staining of cultured HeLa cells treated with nanoparticles (PD, PDB, PDB+HA-scVEGF121 and PDB+HA-EGF) loaded with paclitaxel or direct application of paclitaxel as positive control. Negative control being HeLa cells without addition of paclitaxel.

3.4 Discussion

The purpose of this study is to design an elastin-like polypeptide fused with a α-helix peptide (helixB) in order to favor a heterodimer formation when combined to another α-helix peptide (helixA) fused with a growth factor as constructed previously. The ELP fused with polyaspartic acid sequence and α-helix peptide at its C-terminal induced the formation of nanoparticles. The unfolding and folding state of the nanoparticles appear to respond under temperature change. Moreover, encapsulation of small molecules and drugs seems to occur during the phase transition temperature. In addition to those attributes, HA-scVEGF121 or HA-EGF constructed previously, was combined to the nanoparticles in order to form a non-covalent bonding around the phase transition temperature for targeted drug delivery.

The turbidimetry reveals that PD and PDB nanoparticles are formed as the temperature rises to the phase transition temperature and did not disaggregate during the cooling stage. It validates the self-assembly of our fusion protein [17]. The suspension of PD and PDB particles may have been hampered by the deficiency of water molecules within the amid groups which prompted the stabilization of the folding state [21]. The slow aggregation and disaggregation kinetics of PD explain the difference in paths found between PD and PDB traces [22] this might be explained by the addition of helixB fragment to the original PD backbone. To corroborate previously established findings, 1,8-ANS was loaded into PD and PDB particles to prove their potency in encapsulating drugs within their respective cores.

In Figure 6, a strong increase in fluorescence was observed at 50 °C, which coincided approximately with the phase transition of the nanoparticles that encapsulated the fluorophore within its hydrophobic core. Similar results have been observed using 1,8-ANS as a fluorescent probe, which registered emission intensity in the presence of hydrophobic surfaces within tightly folded proteins [23-25]. In addition, relatively high fluorescence emissions were recorded even after cooling treatment, however, they remain slightly lower than those at 50 °C. In both cases, the fluorescence intensity of PD is somewhat lower than that of PDB. These findings imply that the folding of the nanoparticles remained stable and was not affected by the temperature variation following the particle formation and only insignificant amount of particles were unfolded. Thus, the

ELP-poly(aspartic) sequences are thermo-sensitive prior to particle formation and thermo-resistance subsequently. This also suggests that the fusion proteins are hydrophilic and have a stretched out conformation below their phase transition temperatures whereas they become hydrophobic and with a crumpled conformation above their phase transition temperature [26]. The additional helixB sequence added to the ELP-poly(aspartic) sequences did not impede the activity of the nanoparticle formation nor their thermo-responsive property.

TEM examination shows spherical-shaped granulations. The particle amount at 25 °C differs from the particles heated at 50 °C. Despite the usage of same concentration, the number of folded PD at 50 °C appear fewer than PDB. This might be explained by the helixB addition, which might prompt the folding process.

To verify the genuine efficacy of PDB in comparison with PD, HA-scVEGF$_{121}$ was initially reacted with PDB to confirm the heterodimer formation between helixA and helixB. Figure 7 showed that heterodimer formation occurs and that is explained by the electrostatic destabilization of the homodimers.

Cell staining results demonstrate that cells treated with PD, PDB and especially PDBE and PDBV scored considerable cell death on day 2 and day 4 compared with positive control, where a direct application of PTX on cells was applied. PD and PDB seem to have attached to the cell surface in an unspecific manner. PDBE and PDBV appear to have been recognized by cell receptors located on cell surface EGF-R and VEGF-R respectively. This is described by the significant cell death that has been detached and removed from cell media after washing phase. The application of PDBE in addition to PDBV was only for receptor recognition confirmation since only few studies apply VEGF for therapeutic applications. It confirms that EGF, VEGF and their receptors for cancer therapy applications [27, 28]. An unpredicted fact was observed; cells in dishes treated with the same fusion proteins mentioned previously have been massively detached, particularly those treated with PDBE and PDBV. The phenomenon remains inexplicable. Hypothesis suggests that the presence of coiled-coil structure combined with targeted drug delivery might act as tumor suppressor that might result in inhibiting cell surface polarity and adhesion and as a result detaching the cell [18]. Another hypothesis supposes that our coiled-coil complex might have acted like a thermo-responsive sheet that worked as a large

drug release unit. Once the drug has been released, the polymers creating the sheet return to their initial extensive conformation by dragging along the dead cells that have been lost their adhesive ability to the plate.

Further investigations need to be performed to confirm previous hypothesis. In addition to what has been proved in this study, coiled-coil approach using nanoparticles might also be used to prevent tumorigenesis by anti-angiogenesis drugs preventing the blood vessels' outgrowth.

3.5 Conclusion

We have successfully developed a new approach for a targeted drug delivery and controlled release using ELP thermo-responsive nanoparticles non-covalently bound to growth factor. Nanoparticles have effectively delivered paclitaxel and induced cell death and detachment. This new strategy established a promising biomaterial for drug delivery.

3.6 References

[1] Soppimath K, Aminabhavi T, Kulkarni A, Rudzinski W. Biodegradable polymeric nanoparticles as drug delivery devices. Journal of controlled release : official journal of the Controlled Release Society 2001;70(1-2):1-20.

[2] Malik DK, Baboota S, Ahuja A, Hasan S, Ali J. Recent advances in protein and peptide drug delivery systems. Current drug delivery 2007;4(2):141-51.

[3] Meenach S, Shapiro J, Hilt J, Anderson K. Characterization of PEG-iron oxide hydrogel nanocomposites for dual hyperthermia and paclitaxel delivery. Journal of biomaterials science Polymer edition 2013;24(9):1112-26.

[4] Jain A, Jain A, Gulbake A, Shilpi S, Hurkat P, Jain S. Peptide and protein delivery using new drug delivery systems. Critical reviews in therapeutic drug carrier systems 2013;30(4):293-329.

[5] Veronese F, Pasut G. PEGylation, successful approach to drug delivery. Drug discovery today 2005;10(21):1451-8.

[6] Pritchard E, Hu X, Finley V, Kuo C, Kaplan D. Effect of silk protein processing on drug delivery from silk films. Macromolecular Bioscience 2013;13(3):311-20.

[7] Liang M, Wang L, Liu X, Qi W, Su R, Huang R, et al. Cross-linked lysozyme crystal templated synthesis of Au nanoparticles as high-performance recyclable catalysts. Nanotechnology 2013;24(24):245601.

[8] Ho H, Nero T, Singh H, Parker M, Nie G. PEGylation of a proprotein convertase peptide inhibitor for vaginal route of drug delivery: in vitro bioactivity, stability and in vivo pharmacokinetics. Peptides 2012;38(2):266-74.

[9] Flenniken M, Liepold L, Crowley B, Willits D, Young M, Douglas T. Selective attachment and release of a chemotherapeutic agent from the interior of a protein cage architecture. Chemical communications (Cambridge, England) 2005(4):447-9.

[10] Ren D, Kratz F, Wang S-W. Protein nanocapsules containing doxorubicin as a pH-responsive delivery system. Small (Weinheim an der Bergstrasse, Germany) 2011;7(8):1051-60.

[11] Kratz F. Albumin as a drug carrier: design of prodrugs, drug conjugates and nanoparticles. Journal of controlled release : official journal of the Controlled Release Society 2008;132(3):171-83.

[12] Klenkler BJ, Griffith M, Becerril C, West-Mays JA, Sheardown H. EGF-grafted PDMS surfaces in artificial cornea applications. Biomaterials 2005;26(35):7286-96.

[13] Boucher C, Ruiz JC, Thibault M, Buschmann MD, Wertheimer MR, Jolicoeur M, et al. Human corneal epithelial cell response to epidermal growth factor tethered via coiled-coil interactions. Biomaterials 2010;31(27):7021-31.

[14] McDaniel J, Callahan D, Chilkoti A. Drug delivery to solid tumors by elastin-like polypeptides. Advanced Drug Delivery Reviews 2010;62(15):1456-67.

[15] Fletcher J, Boyle A, Bruning M, Bartlett G, Vincent T, Zaccai N, et al. A basis set of de novo coiled-coil Peptide oligomers for rational protein design and synthetic biology. ACS synthetic biology 2012;1(6):240-50.

[16] Fujita Y, Mie M, Kobatake E. Construction of nanoscale protein particle using temperature-sensitive elastin-like peptide and polyaspartic acid chain. Biomaterials 2009;30(20):3450-7.

[17] Herrero-Vanrell R, Rincon AC, Alonso M, Reboto V, Molina-Martinez IT, Rodriguez-Cabello JC. Self-assembled particles of an elastin-like polymer as vehicles for controlled drug release. J Control Release 2005;102(1):113-22.

[18] O'Shea EK, Lumb KJ, Kim PS. Peptide 'Velcro': design of a heterodimeric coiled coil. Current biology : CB 1993;3(10):658-67.

[19] O'Shea EK, Rutkowski R, Stafford WF, 3rd, Kim PS. Preferential heterodimer formation by isolated leucine zippers from fos and jun. Science 1989;245(4918):646-8.

[20] Fujita Y, Mie M, Kobatake E. Construction of nanoscale protein particle using temperature-sensitive elastin-like peptide and polyaspartic acid chain. Biomaterials 2009;30(2):3450-7.

[21] Wright E, Conticello V. Self-assembly of block copolymers derived from elastin-mimetic polypeptide sequences. Advanced Drug Delivery Reviews 2002;54(8):1057-73.

[22] Meyer D, Kong G, Dewhirst M, Zalutsky M, Chilkoti A. Targeting a genetically engineered elastin-like polypeptide to solid tumors by local hyperthermia. Cancer research 2001;61(4):1548-54.

[23] Ptitsyn O. Molten globule and protein folding. Advances in protein chemistry 1995;47:83-229.

[24] Kuwajima K. The molten globule state as a clue for understanding the folding and cooperativity of globular-protein structure. Proteins 1989;6(2):87-103.

[25] Semisotnov G, Rodionova N, Razgulyaev O, Uversky V, Gripas A, Gilmanshin R. Study of the "molten globule" intermediate state in protein folding by a hydrophobic fluorescent probe. Biopolymers 1991;31(1):119-28.

[26] Choi BG, Song R, Nam W, Jeong B. Iron porphyrins anchored to a thermosensitive polymeric core-shell nanosphere as a thermotropic catalyst. Chem Commun (Camb) 2005(23):2960-2.

[27] Dudu V, Rotari V, Vazquez M. Targeted extracellular nanoparticles enable intracellular detection of activated epidermal growth factor receptor in living brain cancer cells. Nanomedicine : nanotechnology, biology, and medicine 2011;7(6):896-903.

[28] Ban H, Uno M, Nakamura H. Suppression of hypoxia-induced HIF-1alpha accumulation by VEGFR inhibitors: Different profiles of AAL993 versus SU5416 and KRN633. Cancer letters 2010;296(1):17-26.

Chapter 4

General conclusion and future perspectives

"I think and think for months and years. Ninety-nine times, the conclusion is false. The hundredth time I am right." – Albert Einstein

4.1 General conclusion

The synthesis of an elastin-like biomaterial has revolutionized the tissue engineering and drug delivery system fields. The biodegradable, biocompatible and non-immugenic features conferred flexible applications on ELPs. Nevertheless, ELPs demonstrated outstanding findings when conjugated to DNA, proteins or polymers. Their potency in mimicking different platforms such as hydrogels and nanoparticles overcame challenges in releasing growth factors and drugs.

Tethering growth factors to ELPs have proved to bestow specific targeting. Hence, the purpose of this thesis was the design of new biomaterials for both tissue regeneration and drug delivery system. The originality of this work consisted of using a set of coiled-coil proteins, helixA and helixB, as non-covalent binding between ELPs and growth factors. In addition, the designed fusion proteins acquired biologically active attributes that also attach to hydrophobic surfaces and bind with site-specific manner.

In chapter 2, we describe the construction of an extracellular matrix fusion protein formed by collagen binding domain, RGD, IKVAV, elastin-like polypeptide and helixB aiming at controlling the activity and the release of the growth factor fusion protein helixA-scVEGF$_{121}$. Our ECM fusion protein (CBDEREI2-helixB) showed high affinity to the low antigenic collagen. Besides, the helixA-scVEGF$_{121}$ promoted greater cell proliferation in its free form than the commercial VEGF. When CBDEREI2-helixB and helixA-scVEGF$_{121}$ were immobilized, tubular formation has been monitored. Synergic effect of non-covalent immobilization of three different angiogenesis upregulating growth factors showed even greater tubular network. This strategy of using coiled-coil binding with helixA/helixB allows the co-immobilization of as many growth factors as needed for an optimum cell growth. Cell differentiation has also been confirmed by high expression of Ang-2.

On the contrary, in chapter 3, a different use of the coiled-coil peptides has been shown. In fact, instead of promoting cell proliferation using helixA-scVEGF$_{121}$, cell specific delivery was expected. Moreover, cancer cells overexpress VEGF receptors; therefore, helixa-VEGF$_{121}$ has been exploited as drug delivery target. PTX has been loaded

within ELP-based nanoparticles fused with helixB. At transition temperature, the coiled-coil complex forms simultaneously with the folding of ELP-helixB into nanoparticles. Unlike the PVGV repeats where the inverse transition is completely reversible, the PAVGV repeats forming the present ELPs do not unfold during cooling treatment. This strategy guarantees proper drug delivery to cells and consequently, proper drug release. The non-covalent immobilization of ELPs and growth factors demonstrated that in addition to drug release, cell death and detachment has been noticed in an identical way than the direct application of PTX on HeLa cells.

The three kinds of fusion proteins designed in this study: ELP-based ECM and nanoparticle fusion proteins and growth factor proteins provide with an innovative approach in tissue engineering and drug delivery system. These methods are easy to synthesis and offer a great flexibility in use according to targeted tissues (i.e., nervous tissues, osseous tissues). The non-covalent immobilization methodology of these fusion proteins showed practical applications in two complete distinct fields.

4.2 Future perspectives

The use of non-covalent method especially the coiled-coil complex prompted our interest into developing a bigger complex, in other words, constructing a network encompassing different fusion proteins. In actual fact, literature recommends the synergistic effect of two or more growth factors in case of tissue regeneration. The thought of designing a growth factor (GF) fused with helixA at its N-terminus and C-terminus (hA-GF-hA) would lead the fusion protein to bind to two different compounds. For instance, the complex hA-GF-hA would bind to an ECM-hB fusion protein at one side and to another GF-hA fusion protein at another side and so on and so forth.

The design of this multi-complex micelle might be a good candidate to control growth factor release and to provide with the tissue a biological support. As for the drug delivery system, cancer cells express multi-growth factor receptors rendering it difficult to target drugs onto these cancer cells. Therefore, immobilizing non-covalently ELP-helixB

nanoparticles with multiple growth factor fusion proteins might facilitate targeting approaches for an efficient drug delivery.

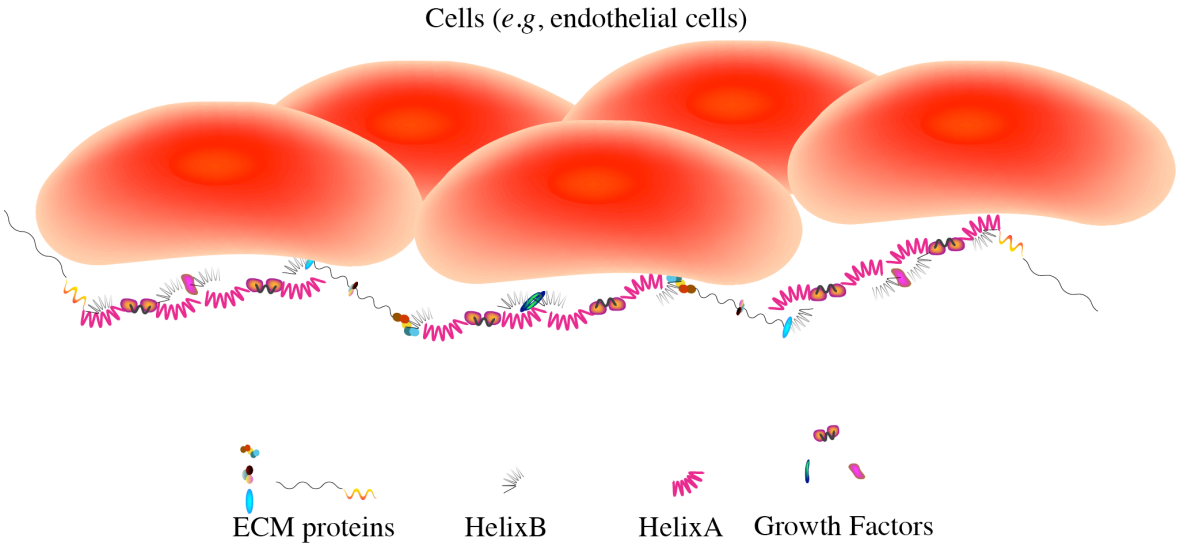

Schematic representation of a possible micelle formation using coiled-coil binding after tagging helixA or helixB on both sides of an ECM protein or growth factor protein.

List of publication

Peer reviewed

- **Assal Y**, Mie M, Kobatake E. The promotion of angiogenesis by growth factors integrated with ECM proteins through coiled-coil structures. Biomaterials 2013;34(13):3315-23.

Conference/Symposium

Communication - Oral

- **Assal Y**, Mie M, Kobatake E, Construction of Vascular Endothelial Growth Factor Fusion Protein that promotes Angiogenesis, International Graduate Forum on Biotechnology, Bioengineering and Biomedical Science, Beijing, China, August 2011

Communication – Poster

- **Assal Y**, Mie M, Kobatake E, Construction of ECM-growth factor integrated protein through coiled-coil structure to promote angiogenesis, 3rd World Congress in Tissue Engineering and Regenerative Medecine TERMIS, Vienna, Austria, September 2012

Publication

- **Assal Y**, et al., Construction of ECM-growth factor integrated protein through coiled-coil structure to promote angiogenesis, J Tissue Eng Regen Med 2012; 6 (Suppl. 1): 1-429

Academic Award

- Akaike Journal Award (赤池ジャーナル賞) Tokyo Institute of Technology, February 2013

Aknowledgments

In completion of this work and first and foremost, I express my profound gratitude and appreciation to my supervisor Prof. Eiry Kobatake for his valuable suggestions, encouragement, and moral support. I would like to thank him for giving me the opportunity to work under his guidance and help me completing my research as a graduate student at Tokyo Institute of Technology.

I am also very grateful to Dr. Masayasu Mie for pushing me in investigating beyond my area of expertise. I highly appreciate his valuable suggestions and constructive criticism. With different backgrounds and unique interests, I have had the opportunity to learn much about science and engineering from each of them. In common was their unfailing kindness not only as researchers but also as individuals. They have been of a huge help during hard times such as the 2011 earthquake by translating and forwarding information regarding the situation. 本当に…ありがとうございました。

My TITech life was made enjoyable in large part due to the many friends and colleagues, past and present, at Kobatake Laboratory for their support and friendship. A special note of thanks to Imen Elloumi Hannachi who introduced me to Kobatake Lab. Since then, a friendship started over the pacific and she has been ever since my long distance mentor. Thank you. I would like to show my gratitude to Farhima Akter for her help, support and encouragement throughout my research work. She and her husband Amranul Haque were both inspiring and enthusiastic scientists and friends. Thank you both. I cannot forget to thank Punpun for being the energy entity of our lab and such a lovely and loveable young scientist.

A good support structure is important to surviving and staying sane in grad school. A big thank you to Vipul Gupta who, to be honest, didn't give me a break about science, even our lunch talks always ended up talking about proteins, DNA and protocols. He is one of the rare true scientists I have met so far. He has been of a great moral support the last six months. It definitely helps to have a buddy going through the same Ph.D. insanity. Thank you Vip for your time and patience.

I was lucky to be part of the Central Sport Nagatsuta Swimming team. I would like to thank the team members for the memorable training sessions and laughter we shared afterwards. Not only they have been a second family but also thanks to them, my Japanese proficiency seems to have slightly improved.

I gratefully acknowledge the funding sources that made my Ph.D. work possible. I was funded by Grants-in-aid for Scientific Research from the Ministry of Education, Culture, Sports, Science and Technology of Japan and JSPS Institutional Program for Young Researcher Overseas Visits.

I can't thank enough my best friend Sahar Mejri for her endless moral support. We've been there for one another and have taught each other and ourselves how to see the glass half-full. I know that when we are old, Sahar will still be there as a smiling, supportive and caring friend. Thank you.

Finally, I thank my mom, dad and especially my sister for her presence these last three months. My parents have sacrificed their lives for my sister and myself proving unconditional love and constant care. I wouldn't have made it this far without them. Despite the distance, they have been supportive and encouraging in all my pursuits. I love you.